Assessment of High-Heat-Flux Thermal Management Schemes

Issam Mudawar

***Abstract*—This paper explores the recent research developments in high-heat-flux thermal management. Cooling schemes such as pool boiling, detachable heat sinks, channel flow boiling, microchannel and mini-channel heat sinks, jet-impingement, and sprays, are discussed and compared relative to heat dissipation potential, reliability, and packaging concerns. It is demonstrated that, while different cooling options can be tailored to the specific needs of individual applications, system considerations always play a paramount role in determining the most suitable cooling scheme. It is also shown that extensive fundamental electronic cooling knowledge has been amassed over the past two decades. Yet there is now a growing need for hardware innovations rather than perturbations to those fundamental studies. An example of these innovations is the cooling of military avionics, where research findings from the electronic cooling literature have made possible the development of a new generation of cooling hardware which promise order of magnitude increases in heat dissipation compared to today's cutting edge avionics cooling schemes.**

***Index Terms*—Avionics cooling, electronic cooling, flow boiling, high heat flux, jet-impingement cooling, liquid-immersion cooling, microchannel heat sinks, pool boiling, spray cooling.**

I. Introduction

A. High-Flux and Ultra-High-Flux Cooling Needs

BREAKTHROUGHS in many of today's cutting-edge technologies are becoming increasingly dependent upon the ability to safely dissipate enormous amounts of heat from very small areas. Two ranges of heat flux can be loosely identified relative to the magnitude of the heat dissipation and the type of coolant permissible in a particular application. These are the *high-flux* range, with cooling heat flux requirements on the order of 10^2–10^3 W/cm^2, and the *ultra-high-flux* range, with heat fluxes of 10^3–10^5 W/cm^2.

The high-flux range is presently encountered in high performance supercomputers, power devices, electric vehicles, and advanced military avionics. The stringent material and electrical compatibility requirements in these applications prohibit the use of water in direct contact with current-carrying components; hence the need to use low boiling point dielectric fluorochemical coolants such as those developed by the 3M Company. Collectively known as "Fluorinerts," these inert fluids have a wide range of applications including liquid chromatography, precision reflow soldering, leak and thermal shock testing of electronic components, and cooling of high power devices. For two-phase electronic cooling, the most promising of the Fluorinerts are FC-87, PF-5052 and FC-72 which, at atmospheric pressure, have saturation temperatures of 32.0, 50.0 and 56.6°C, respectively. These temperatures are low enough to maintain moderate device temperatures but high enough to permit discharge of the heat to an ambient air stream. Table I shows the thermophysical properties of these compounds, especially specific heat and latent heat of vaporization, are far inferior to those of water. Several techniques are therefore required to boost their cooling potential to meet the cooling requirements of high-flux devices. Another drawback with these coolants is environmental

TABLE I
SATURATED THERMOPHYSICAL PROPERTIES OF DIFFERENT LIQUID COOLANTS AT 1 atm

Fluid	Saturation temperature T_{sat} (°C)	Liquid density ρ_f (kg m^{-3})	Liquid specific heat $c_{p,f}$ (J kg^{-1} K^{-1})	Vapor density ρ_g (kg m^{-3})	Latent heat of vaporization h_{fg} (kJ kg^{-1})	Surface tension $\sigma \times 10^3$ (N m^{-1})
FC-72	56.6	1600.1	1102.0	13.43	94.8	8.35
FC-87	32.0	1595.0	1060.0	13.65	87.93	14.53
PF-5052	50.0	1643.2	936.3	11.98	104.7	13.00
Water	100.0	957.9	4217.0	0.60	2256.7	58.91

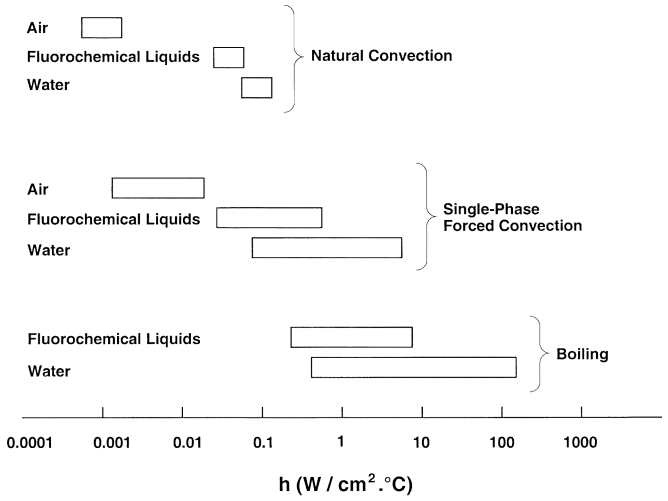

Fig. 1. Heat transfer coefficients attainable with natural convection, single-phase liquid forced convection and boiling for different coolants.

Manuscript received November 16, 2000; revised March 22, 2001. This work was recommended for publication by Associate Editor K. Ramakrishna upon evaluation of the reviewers' comments. This work was presented at the 7th Intersociety Conference on Thermal, Mechanical, and Thermomechanical Phenomena in Electronic Systems (ITHERM 2000), Las Vegas, NV, May 23–26, 2000. This work was supported by the Office of Basic Energy Sciences, U.S. Department of Energy (Grant DE-FG02-93ER14394.A003), the National Science Foundation, U.S. Navy, U.S. Air Force, IBM, 3M Company, and General Electric Company.

I. Mudawar is with the Purdue University International Electronic Cooling Alliance (PUIECA), School of Mechanical Engineering, Purdue University, West Lafayette, IN 47907 USA.

Publisher Item Identifier S 1521-3331(01)04792-4.

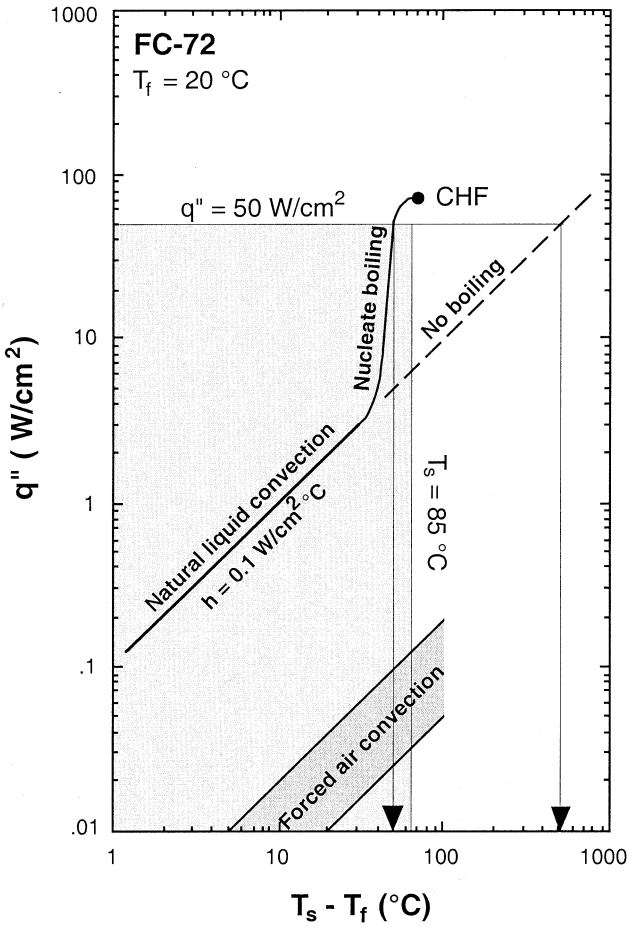

Fig. 2. Comparison of cooling characteristics with boiling compared to natural convection in liquid and to forced air convection.

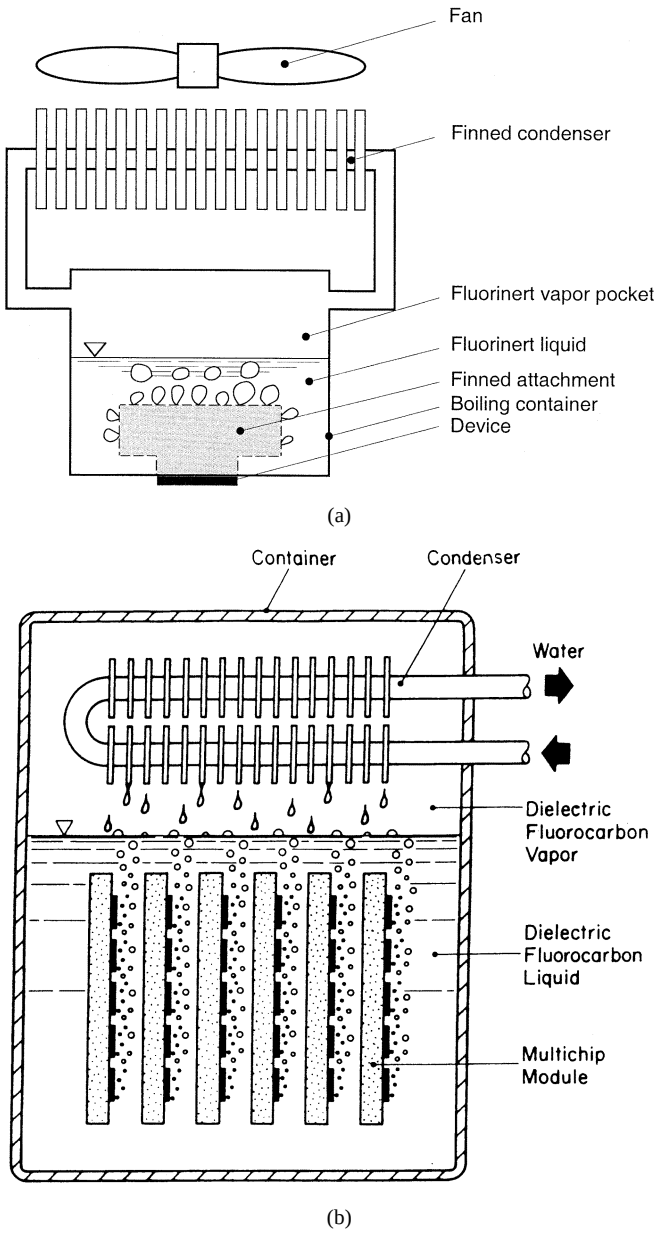

Fig. 3. (a) Air-cooled thermosyphon for a single processor. (b) Thermosyphon for cooling of several multichip modules.

impact. While the absence of chlorine atoms from Fluorinerts renders them less harmful to the ozone layer than their dielectric predecessors (e.g., Freon 113), there is some concern over the global warming potential of all fluorochemical coolants, as well as the danger of chemical breakdown and production of harmful substances upon exposure to high temperatures.

Ultra-high-fluxes are encountered in numerous high-energy devices. Fusion reactors, for example, contain components that require continuous cooling on the order of 10^4 W/cm^2 [1]. Other examples are directed energy devices such as high-efficiency, multimegawatt continuous-wave magnetrons used for short-pulse lasers and radars, and synchrotron sources that deliver high brilliance x-ray beams. These synchrotron beams possess unprecedented power densities, some as high as 1.5×10^4 W/cm^2 [2]. The enormous cooling requirements of these high-energy devices preclude the use of fluorochemical coolants. For these applications, water remains the coolant of choice because of its superior thermophysical properties, abundance, and low cost.

B. Phase-Change Cooling

Fig. 1 shows the range of heat transfer coefficients attainable with different fluids and cooling schemes. Air is the most affordable, and remains the most widely used coolant for most applications. However, the poor thermal transport properties of air greatly reduce its cooling potential, limiting its use to low heat flux devices. Better results are possible with fluorochemical liquids, while the most demanding cooling situations are typically managed with water. Fig. 1 shows forced convection can greatly improve cooling performance relative to natural convection for all coolants. However, superior performances require a change-of-phase (boiling) of the liquid coolant.

Liquid cooling can be employed with or without boiling. Fig. 2 shows how boiling can greatly reduce the device temperature compared to single-phase liquid cooling. For electronic cooling, phase change requires the use of a coolant that boils 10 to 40°C below the desired device operating temperature. Fig. 2 shows the relationship between the device heat flux and device temperature measured experimentally in Fluorinert FC-72 at 20°C [3]. Single-phase natural convection cooling prevails for device heat fluxes up to 3 W/cm^2, yielding close

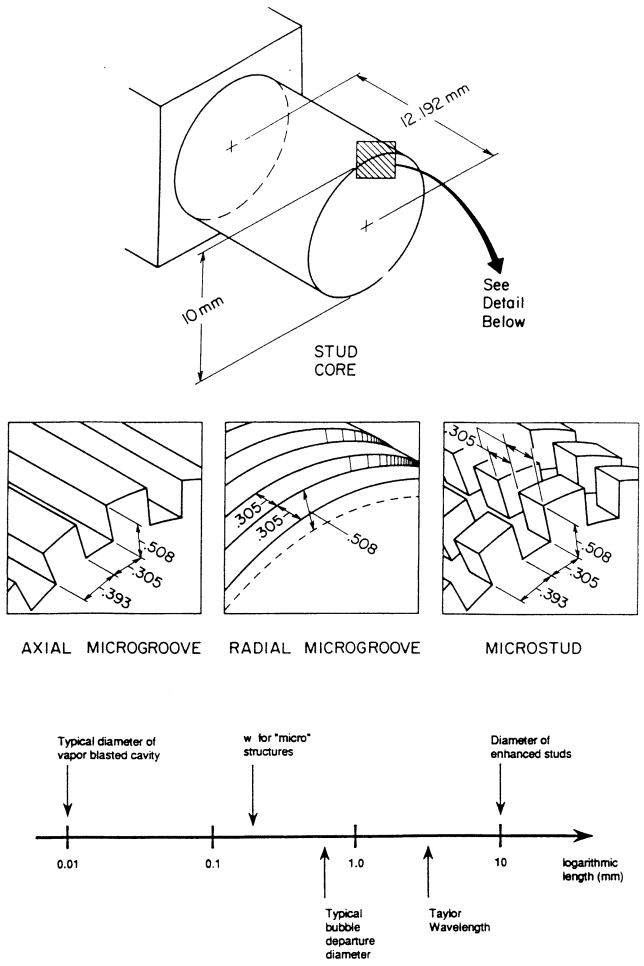

Fig. 4. High-performance extended surfaces incorporating different forms of surface enhancement [16].

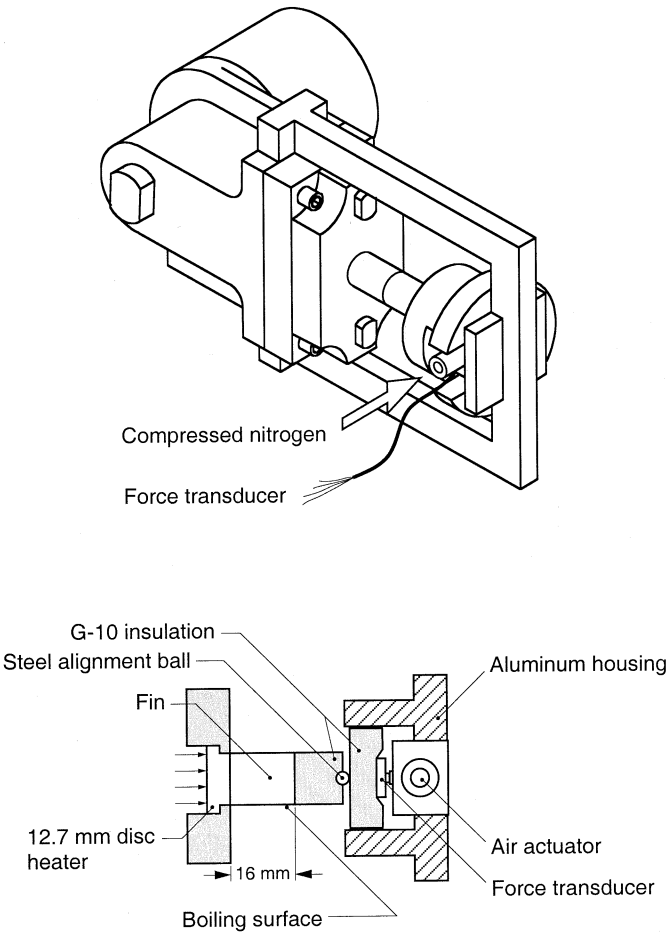

Fig. 5. Press-on fin test assembly.

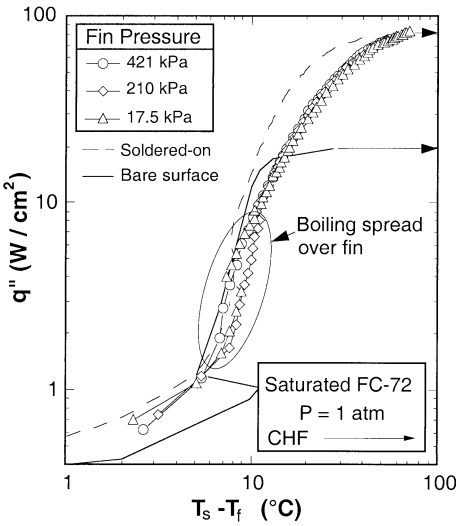

Fig. 6. Boiling curves for different press-on fin pressures compared to those of soldered-on fin and bare surface (adapted from [18]).

to a linear increase in device temperature with increasing heat flux. Boiling requires that the device temperature exceed the saturation temperature of Fluorinert liquid (56°C for FC-72). The liquid adjacent to the device surface has to be superheated by a few degrees above the saturation temperature for the first bubbles to begin forming at and departing from the device surface. Higher heat fluxes increase this superheat, causing bubbles to form over a greater fraction of the device surface area. The bubble growth and departure occur at very high frequencies, constantly drawing bulk liquid toward the device surface. This liquid is then superheated at a very fast rate and begins forming new bubbles to replace the ones just released. These processes of liquid micro-pumping action, transient heat diffusion into the liquid, and ensuing latent heat exchange are responsible for the enormous cooling effectiveness realized with all phase change cooling techniques. These processes also explain a key advantage of phase change: *producing only modest increases in device temperature corresponding to large increases in heat flux*. As shown in Fig. 2, were single-phase cooling to persist above 3 W/cm^2, the device temperature, T_s, could reach 525°C at 50 W/cm^2 compared to only 70°C with boiling! Phase change makes it possible to dissipate the maximum desired operating heat flux of this particular device of 50 W/cm^2 while maintaining the device safely below the well-established industry limit of 85°C (shaded area in Fig. 2). Fig. 2 also illustrates the remarkable improvements in cooling performance attainable with liquid cooling, with or without phase change, compared to air cooling [4].

One key concern in the implementation of phase-change cooling schemes using dielectric coolants is the uncertainty

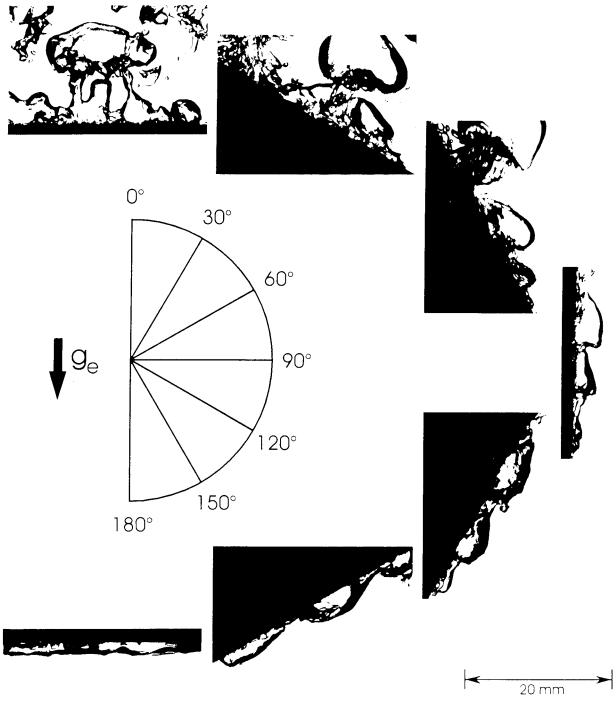

Fig. 7. Pool boiling CHF in saturated Fluorinert PF-5052 at various surface orientations [27].

surrounding the initiation of nucleate boiling. Heat flux levels corresponding to the cessation of boiling when decreasing the device heat flux are often much smaller than those encountered at the onset of boiling when increasing the device heat flux. In other words, boiling incipience often occurs at temperatures much higher than expected, and the excess superheat may quickly be dissipated by vigorous boiling resulting in potential damage to the device by thermal shock. As discussed later in this paper, researchers have developed many different types of surface augmentation techniques to lessen this so-called "incipience temperature drop."

The vapor–liquid exchange process that is responsible for much of the cooling effectiveness realized with phase change requires uninterrupted liquid access to the device surface. Higher heat flux fluxes are dissipated by the production of more vapor bubbles per unit surface area. Unfortunately, this bubble crowding leads to significant vapor coalescence that eventually begins to restrict the liquid access to the device surface. Once the vapor–liquid exchange process in interrupted, the power dissipated in the device itself will no longer be rejected and the device temperature begins to escalate uncontrollably. This is the upper-most point in the boiling curve shown in Fig. 2 and is termed the *critical heat flux* (CHF). *CHF, therefore, constitutes the upper heat flux design limit for any phase-change cooling system.*

This paper explores several methods for implementing phase-change cooling schemes for thermal management of high-flux and ultra-high-flux applications. Much of this work is based on a 16-year initiative at Purdue University to compare different cooling schemes using similar coolants and operating conditions.

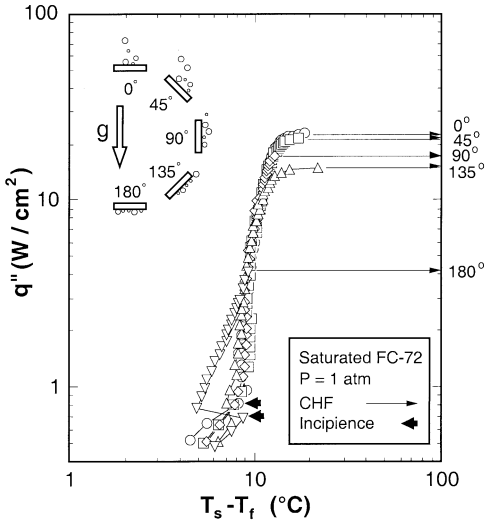

Fig. 8. Pool boiling curves for a 12.7-mm heated disc in saturated FC-72 at different surface orientations (adapted from [18]).

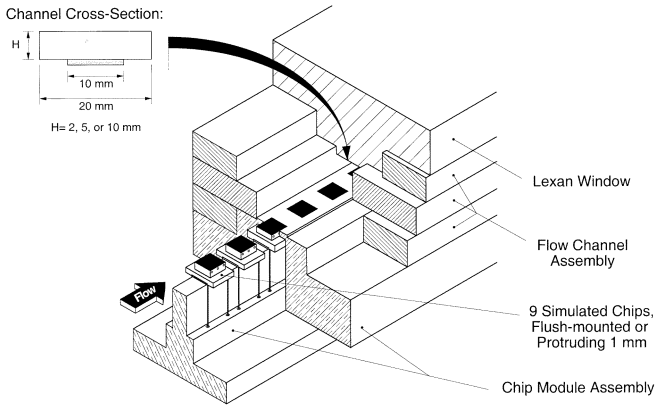

Fig. 9. Multichip channel flow boiling test section.

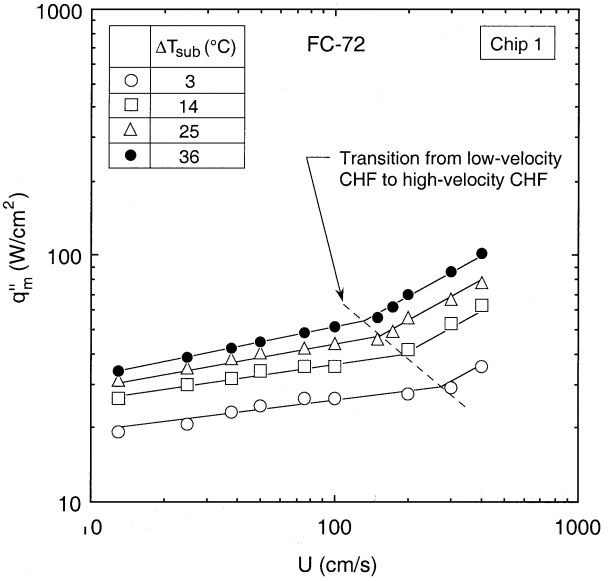

Fig. 10. Channel flow boiling CHF for upstream chip in nine-chip array versus velocity for different subcoolings in vertical upflow (adapted from [33]).

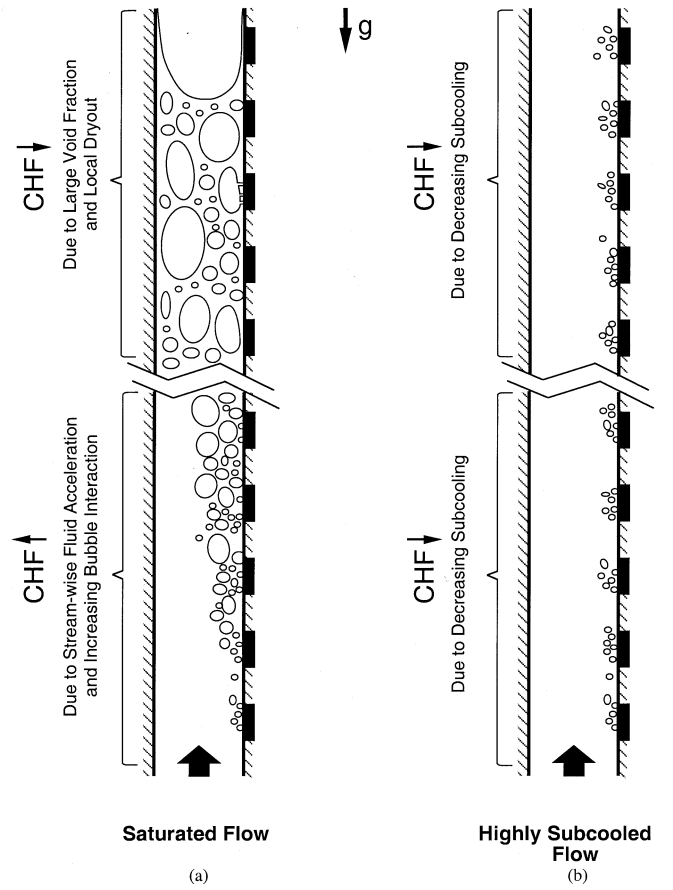

Fig. 11. Multichip channel flow boiling CHF trends for (a) saturated and (b) highly subcooled vertical upflow.

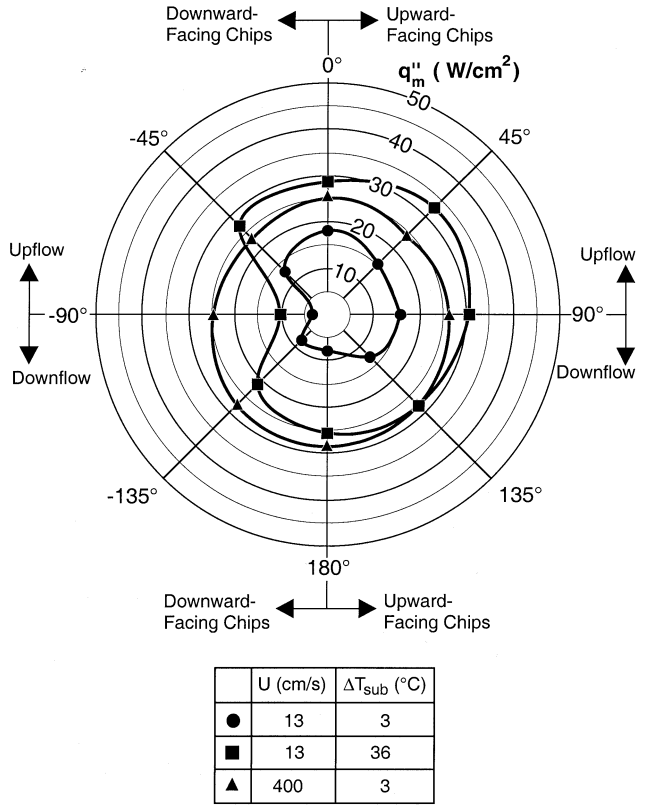

Fig. 12. Polar representation of velocity and subcooling effects on channel flow boiling CHF for different flow orientations (adapted from [38]).

II. Phase Change Cooling Schemes

A. Pool Boiling/Thermosyphons

Implementation: Pool boiling is commonly employed in passive cooling systems called thermosyphons that rely upon buoyancy forces to circulate a dielectric coolant inside a sealed container. Thermosyphons can be implemented in a broad variety of cooling system shapes and sizes, from those intended to cool a single processor using an air cooled condenser, Fig. 3(a), to much larger systems capable of dissipating large amounts of heat from several muti-chip modules, Fig. 3(b). Inside the thermosyphon, the devices are submerged in a pool of dielectric liquid. The heat dissipated in the devices produces vapor bubbles which are driven by buoyancy forces into the upper region of container, where the vapor condenses and drips back into the liquid pool. Thermosyphons offer several advantages over other electronic cooling systems including passive circulation, ease of fabrication, and the ability to dissipate high heat fluxes when implemented with surface enhancement.

Recent studies (see [5]) have demonstrated various means of enhancing the performance of thermosyphons including:

1) geometrically modifying the chip surface (surface enhancement),
2) subcooling the coolant to a temperature well below the boiling point, and
3) increasing coolant pressure.

Incipience Temperature Drop: Thermodynamic and mechanical equilibrium on a curved vapor–liquid interface requires a certain superheat (excess temperature above the liquid saturation temperature), inversely proportional to the radius of curvature of the interface, to maintain a given curvature. The minimum superheat required for a bubble to grow from a surface cavity is inversely proportional to the smallest radius that the vapor embryo attains during the stages of bubble growth. Initial vapor embryo size is related to both the liquid-surface contact angle and the cavity angle. For less-wetting fluids, which trap large embryos, the smallest radius is the cavity mouth radius. However, dielectric fluids have very small contact angles (less than one degree for both FC-87 and FC-72 with most materials) [3]. This means large surface cavities that would serve as embryo entrapment sites for less-wetting fluids will flood and vapor embryos are only trapped in microcavities within the visible surface cavities. Because the size and geometry of these microcavities are unknown, prediction of boiling incipience is difficult with most dielectric coolants. Furthermore, the small radius of these microcavities often delays bubble nucleation to relatively high superheats. In one study, bubble nucleation on a polished silicon heater surface in FC-72 was delayed to a surface temperature 46°C higher than the fluid saturation temperature [6].

When boiling finally begins, bubble growth from one cavity can extend into neighboring ones, causing activation of those cavities. The frequent result is that boiling spreads rapidly over

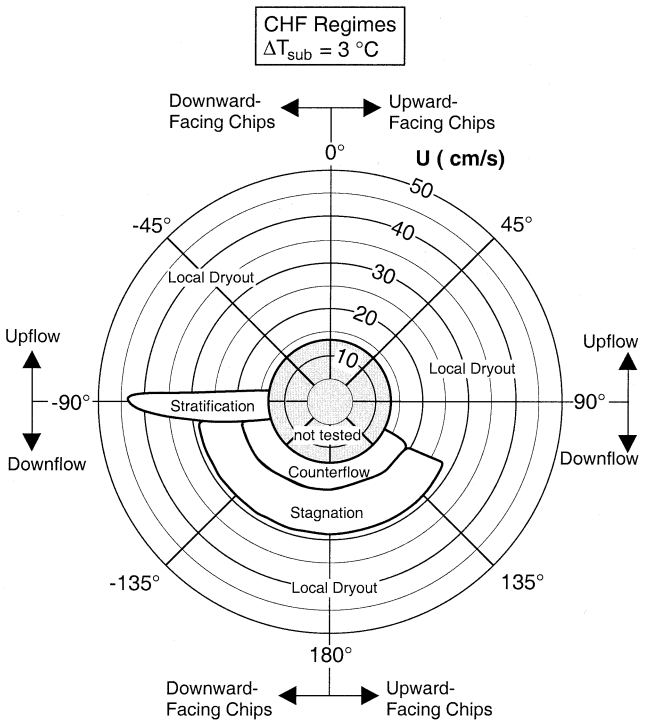

Fig. 13. Polar plot of channel flow boiling CHF regimes for near-saturated FC-72 channel flow boiling at different orientations (adapted from [39]).

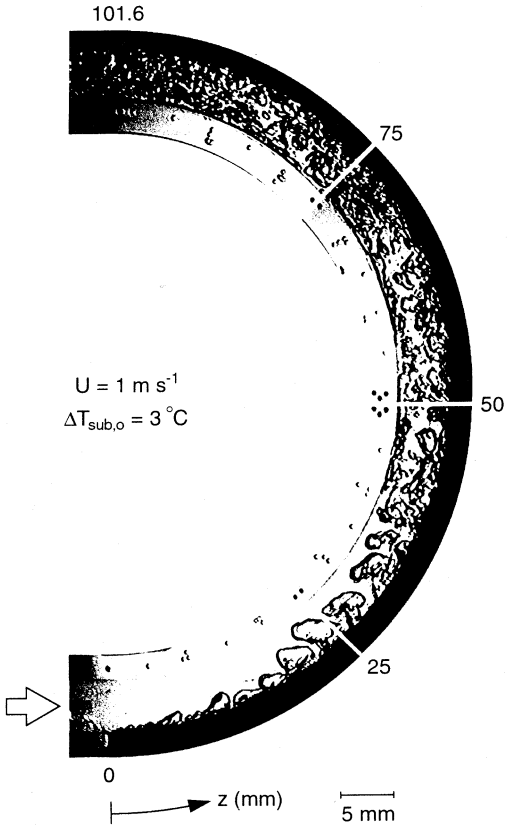

Fig. 14. CHF in flow boiling of FC-72 in a curved channel at 1 m/s (adapted from [49]).

the entire surface, increasing the convection coefficient and extracting enough heat to decrease the surface temperature dramatically. This decrease in temperature, known as the incipience temperature drop, constitutes a thermal shock to the electronic device that can seriously limit its life. Preventing this phenomenon remains a key concern in the implementation of all phase-change schemes in electronic cooling.

Many well-known commercial surfaces that are designed to promote bubble nucleation [7] have been tested in dielectric coolants to explore this phenomenon. Examples include those having porous surfaces (Union Carbide, HIGH-FLUX), re-entrant grooves (Wielanderke AG, GEWA-T), and surfaces formed by bending notched fins to form porous cover plates with subsurface tunnels (Hitachi, THERMOEXCEL-E). Pool boiling experiments by Bergles and Chyu [8] and Marto and Lepere [9] showed the incipience temperature drop in FC-72 was more pronounced for all these surfaces than for smooth surfaces. Efforts in recent years have been focused more on developing re-entrant cavities on a silicon substrate to prevent the incipience temperature drop [10]–[12]. A more comprehensive review of this topic can be found in [3].

Surface Enhancement: Dielectric coolants such as FC-87 and FC-72 possess relatively poor thermal transport properties, and their CHF for bare surfaces is only around 20 W/cm^2 [3]. This falls far below predicted heat flux requirements for many devices and makes surface enhancement for these fluids a necessity.

Many surface enhancement techniques are possible with pool boiling. They include *micro-texturing* the surface with cavities and features whose size and shape are configured relative to the contact angle and thermophysical properties of the coolant [3], [8]–[14]. A second form of surface enhancement is machining of mini-structures (e.g., mini-grooves and mini-studs) which both help sustain the bubble nucleation and increase the surface area available for boiling [3], [5], [15]. The third method of enhancement consists of bonding a relatively large extended surface onto the device surface for the purpose of greatly increasing the heat transfer area, provided the conduction resistance associated with the heat sink does not increase the device temperature appreciably [15], [16].

Mudawar and Anderson [16] demonstrated the feasibility of combining the attractive thermal attributes of different levels of surface enhancement into heat sinks such as those illustrated in Fig. 4. The core of each heat sink is a relatively large copper cylinder whose primary functions are to increase the overall wetted area and the penetration into the bulk liquid outside of the superheated layer adjacent to the base (device surface). Sub-millimeter longitudinal and/or radial grooves are then milled into the stud, and the entire extended surface is finally micro-textured with a blast of silica particles. These heat sinks yielded significant enhancement in CHF, reaching values as large as 105 W/cm^2 and 160 W/cm^2 in saturated and subcooled FC-72, respectively, compared to only 20 W/cm^2 for a bare surface in saturated FC-72. With high subcooling, the liquid is able to absorb a significant fraction of the dissipated heat in the form of sensible heat prior to undergoing phase change. Subcooling also features condensation of vapor bubbles upon departure from the surface, which can aid in preventing massive vapor coalescence along a large multichip module.

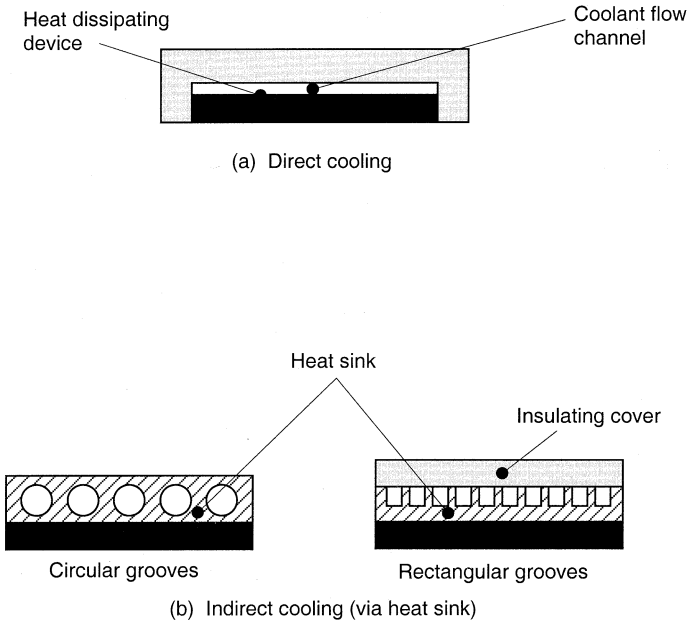

Fig. 15. Microchannel and minichannel flow using (a) direct cooling and (b) indirect cooling.

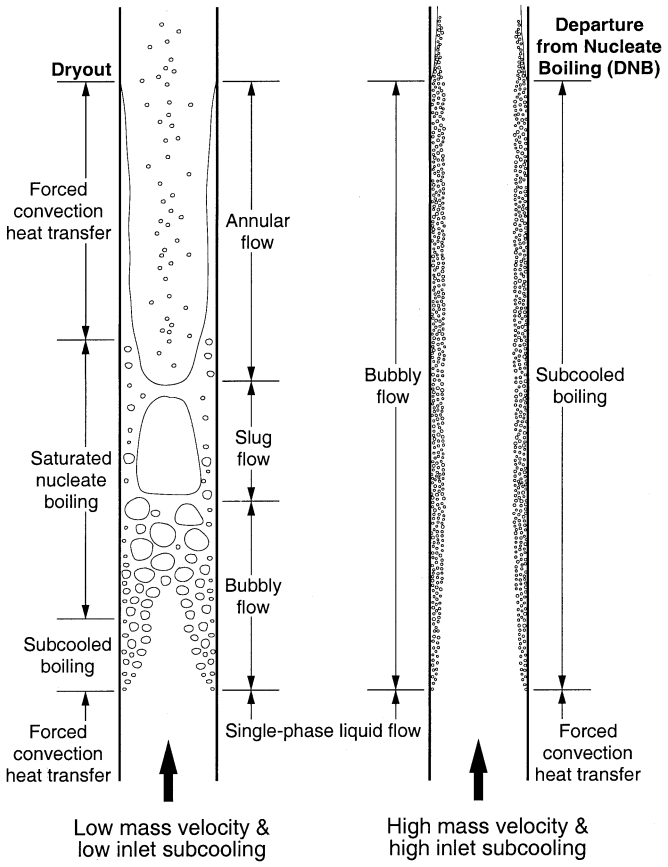

Fig. 16. CHF in microchannels and minichannels corresponding to low mass velocity dryout and high mass velocity DNB.

Press-on Fins: Permanent attachment of a fin to a heat-dissipating device is sometimes an impediment to assembly and maintenance and can reduce component longevity. Additionally, differences in thermal expansion coefficients of the fin and the electronic device material can result in failure of the connection

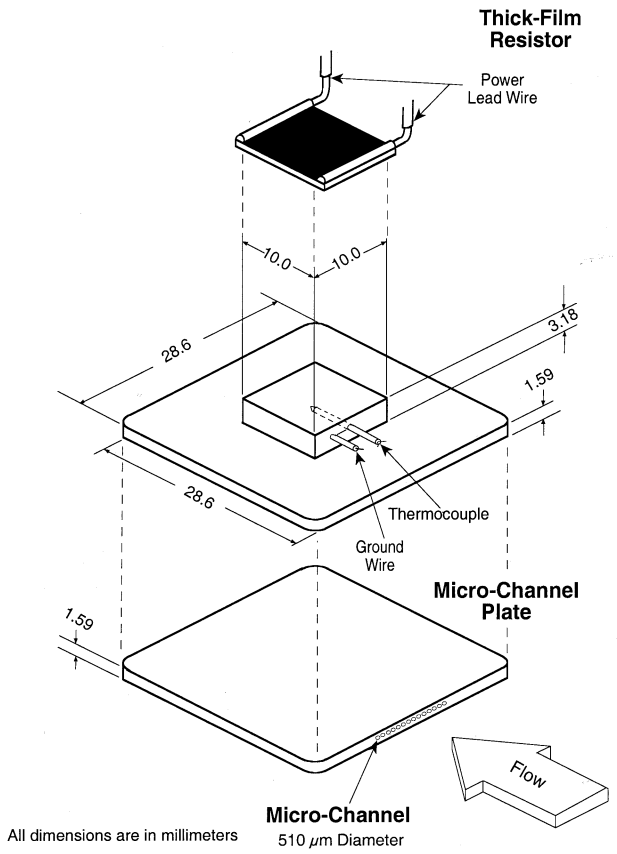

Fig. 17. Microchannel heat sink.

with repeated cycling, eliminating the advantage offered by the fin. Press-on fins with no bonding material have been used before in IBM's indirect water-cooled thermal conduction module (TCM), but they require very close manufacturing tolerances due to the sensitivity of their thermal performance to the effective thickness of the contact gap between the device surface and fin [17].

Highly-wetting dielectric fluids are capable of penetrating extremely small regions and require microcavities for embryo entrapment. Reed and Mudawar [18] capitalized upon this feature by exploring the effectiveness of the crevice at the perimeter of the interface of a heat dissipating device and a pressed-on fin at creating a series of micocavities. Key goals of their study were (a) to utilize the added heat transfer area of the fin to increase CHF, (b) promote early incipience, (c) control the spread of boiling after incipience in a gradual manner, and (d) eliminate the incipience temperature drop commonly observed on bare devices. Tests were conducted in saturated FC-72 and FC-87 at atmospheric pressure for a range of contact pressures using the apparatus illustrated in Fig. 5. At the low mechanical contact pressures allowed on electronic components, the thermal contact resistance showed small dependence on constant pressure as shown in Fig. 6. However, even with contact pressures as low as 17.5 kPa and with a nonoptimized cylindrical fin, CHF values of 85 W/cm^2, a four-fold increase compared to a bare surface, were achieved while maintaining low device surface temperatures. The highly-wetting dielectric fluids were able to penetrate the circumferential crevices at the fin base, superheat, and

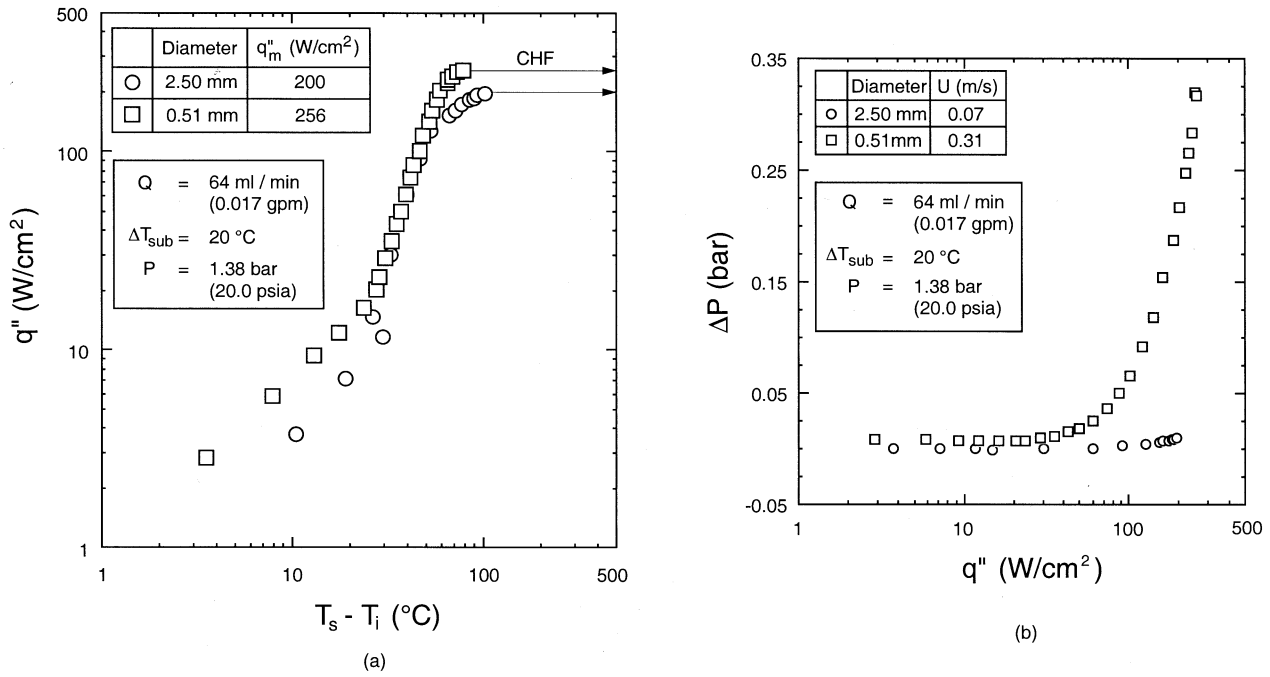

Fig. 18. Comparison of microchannel and minichannel heat sink characteristics relative to (a) cooling performance and (b) pressure drop (adapted from [53]).

nucleate earlier than with a soldered-on fin. This demonstrates the potential of nonpermanent, low-force fins combined with boiling for high performance electronic cooling.

Surface Orientation Effects: The effects of surface orientation on pool boiling heat transfer and CHF have received increased attention during the past three decades because of applications such as nuclear reactor safety, heat treating of metallic parts, and cooling of superconductor coils. The effects of orientation on CHF in electronic cooling are quite unique, given the small size, enclosure volume limitations, and the use of highly wetting dielectric fluids.

Most studies clearly reveal that CHF decreases as surface orientation changes from upward-facing horizontal (0°) to vertical (90°) to downward-facing horizontal (180°) [19]–[25]. Recently, the author and co-workers performed photographic studies of pool boiling in dielectric fluids at different surface orientations in order to ascertain the CHF trigger mechanism associated with each orientation [26], [27]. They concluded that the surface orientations can be divided into three regions: upward-facing (0–60°), near-vertical (60–165°), and downward-facing ($> 165°$), as illustrated in Fig. 7. Each region was associated with a unique CHF trigger mechanism. The vast differences between the observed vapor behavior within the three regions revealed that a single overall pool boiling CHF model cannot possibly account for all the observed orientation effects, but instead three different models should be developed for the three regions. In the upward-facing region, the buoyancy forces remove the vapor vertically off the device surface and can be predicted by the well-known pool boiling CHF model of Zuber *et al.* [28]. The near-vertical region is characterized by a wavy liquid-vapor interface that sweeps along the heater surface. Howard and Mudawar [27] developed a new theoretical model that shows good agreement with CHF data for the entire near-vertical region. In the downward-facing region, the vapor repeatedly stratifies on the heater surface, greatly decreasing CHF. Fig. 8 shows the drastic reduction in CHF as the surface orientation approaches 180°.

A key conclusion from these studies is that electronic devices can be cooled effectively in pool boiling in any orientation between horizontal upward-facing and vertical, but all other orientations placing vapor beneath the device surface should be avoided.

B. Channel Flow Boiling

General Parametric Trends: Packaging of mainframe computers and supercomputers often consists of mounting multichip modules parallel to one another in a compact assembly. Coolant circulated between adjacent modules takes the form of channel flow.

A few researchers have studied direct immersion cooling of electronic devices in channel flow boiling. Their studies encompass such aspects of channel flow boiling as CHF modeling [29], [30], incipience effects of flow parameters [31], [32], chip interactions in multichip modules [33]–[35], chip protrusion [36], [37], and flow orientation [38], [39].

To simulate a multichip channel flow boiling module, the author and co-workers [33]–[35] constructed a linear array of nine heaters which were inserted into a fiberglass plastic test section that formed a rectangular channel as illustrated in Fig. 9. The initial objective of their studies was to determine the parametric effects of CHF relative to flow velocity and subcooling. All chips in the multichip array exhibited similar behavior with increases in velocity and/or subcooling. As shown in Fig. 10, increases in either fluid velocity or degree of subcooling served to increase CHF, but subcooling had a more pronounced effect on CHF at larger velocities. In fact, there appeared to be a transition from a low- to high-velocity CHF regime similar to that observed with an isolated chip [30].

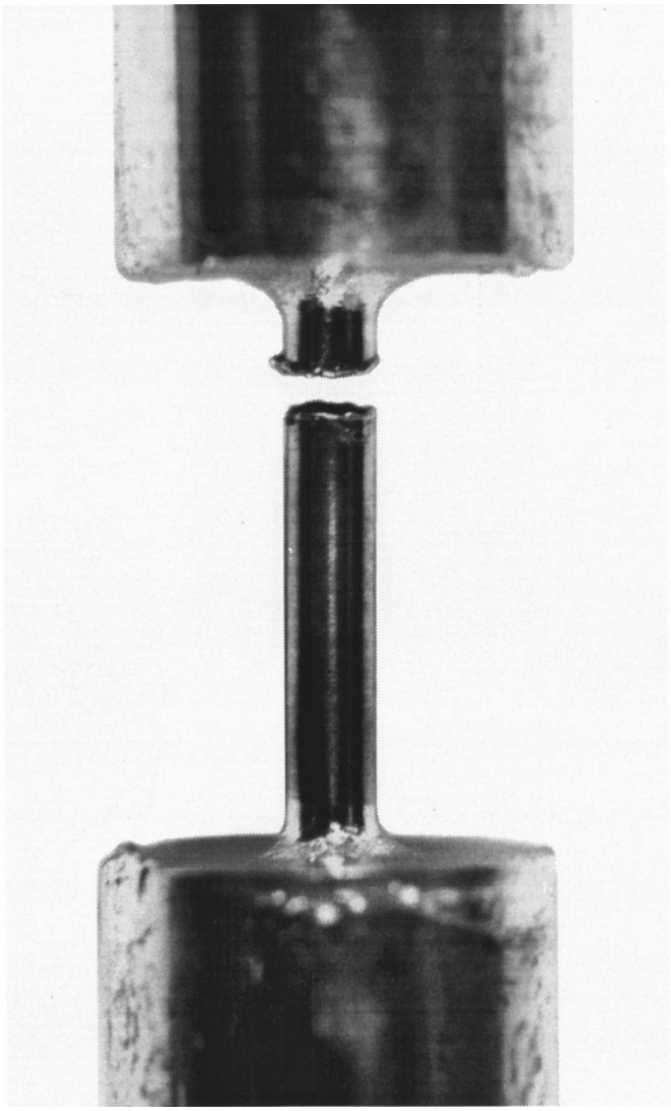

Fig. 19. Microchannel tubular test section after burnout at $27{,}600$ W/cm^2 (adapted from [61]).

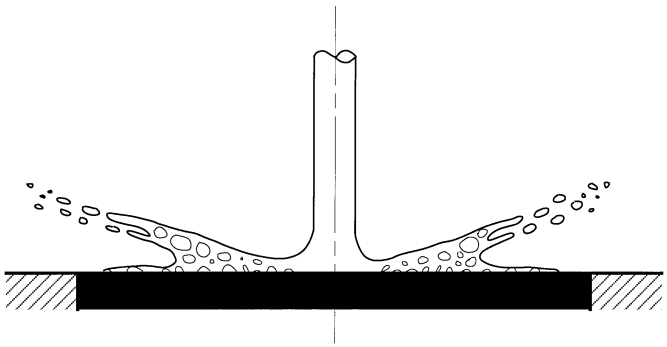

Fig. 20. Liquid wall layer splashing and separation at CHF in free circular impinging jets.

Another objective of these studies was to explore the stream-wise variations in CHF caused by flow interactions between chips. The thermal boundary layer that develops as the coolant passes over the array of heated chips causes a stream-wise increase in the coolant temperature. This effect

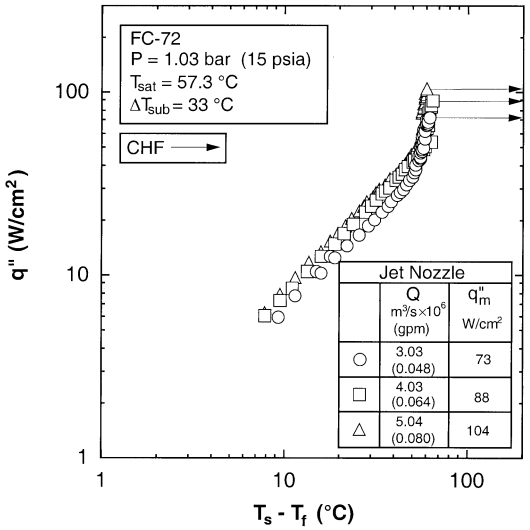

Fig. 21. Free circular jet boiling curves for different flow rates (adapted from [67]).

alone would tend to produce an earlier occurrence of CHF on downstream chips; however, there is also an effect on CHF from bubbles emanating from upstream chips. At near-saturated conditions, downstream chips were observed to be crowded with a substantial population of large bubbles. With increased liquid subcooling, the bubble volume was considerably reduced due to condensation in the cooler bulk liquid. They postulated that at near-saturated conditions, the bubbles emanating from upstream chips serve to increase fluid contact with the downstream chips, thus helping to counterbalance the stream-wise decrease in CHF due to the thermal boundary layer. The increasing vapor void ratio also promotes a stream-wise coolant acceleration which, to a lesser extent, further serves to offset the stream-wise decrease in CHF due to the thermal boundary layer. This process is shown in Fig. 11(a). For the subcooled tests, there was very little interaction between bubble masses formed on adjacent chips and a negligible stream-wise increase in velocity due to phase change; consequently, CHF became mostly sensitive to the stream-wise decrease in local subcooling for downstream chips, as shown in Fig. 11(b).

Flow Orientation Effects: Because of the large density differences between the vapor and liquid phases, body force can play a major role in flow boiling, especially at low coolant velocities, causing such complications as stratification and two-phase flow instabilities [38]–[42]. During stable downflow relative to gravity, vapor bubbles can be entrained in the liquid flow forming a two-phase mixture. One type of unstable downflow is *flooding*, which is characterized by the vapor and liquid moving in opposite directions. This occurs when the buoyancy force acting on the vapor is greater than the drag force exerted by the liquid. The change in vapor motion, from countercurrent at low liquid velocities to co-current at high liquid velocities, passes through a condition called bubble stagnation that occurs when the liquid velocity equals the bubble rise velocity.

In a study of the effects of flow orientation on liquid cooling of mainframe computers and supercomputers, Gersey and Mudawar [38], [39] performed flow boiling experiments using Flu-

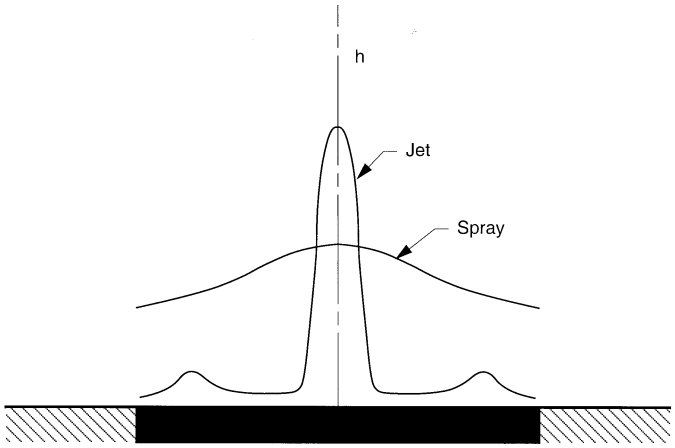

Fig. 22. Qualitative comparison of heat transfer coefficient spatial variations for sprays and free jets.

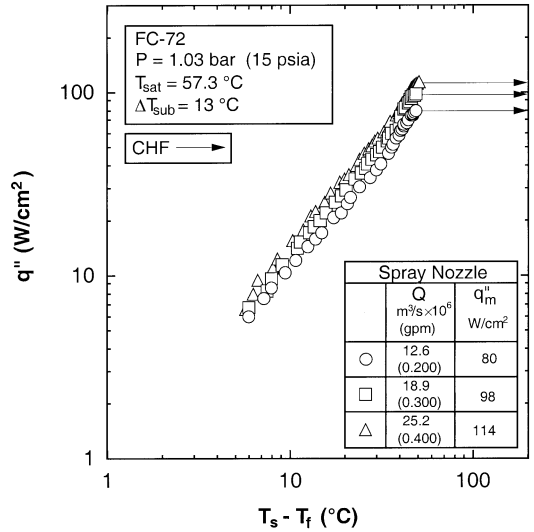

Fig. 23. FC-72 boiling curves for different spray flow rates (adapted from [67]).

orinert FC-72 with a nine-chip array at eight orientations spaced 45-degrees apart. CHF showed significant sensitivity to orientation and, consequently, to the magnitude of the g-field normal to the heated surface. Localized dryout, similar to that observed for vertical upflow, was postulated to be responsible for most of the CHF data. But during the downflow tests at low velocities, CHF was dependent on the relative motion of the liquid and vapor. A polar plot of a sample of the CHF data is presented in Fig. 12. For the case of lowest velocity (13 cm/s) and lowest subcooling (3°C), there was a decrease in CHF with increasing θ (angle of orientation), culminating with the largest decrease at -90 degrees where the vapor separated from the liquid in the channel and formed stratified flow. The absence of liquid contact with the chip surfaces produced an extremely low CHF for this orientation. For the same velocity (13 cm/s) but with a highly subcooled liquid (36°C), the decrease in CHF was much smaller for the upward-facing heater, but CHF still decreased sharply for downflow and downward-facing chip orientations. Overall, increased subcooling served to dampen the effects of orientation

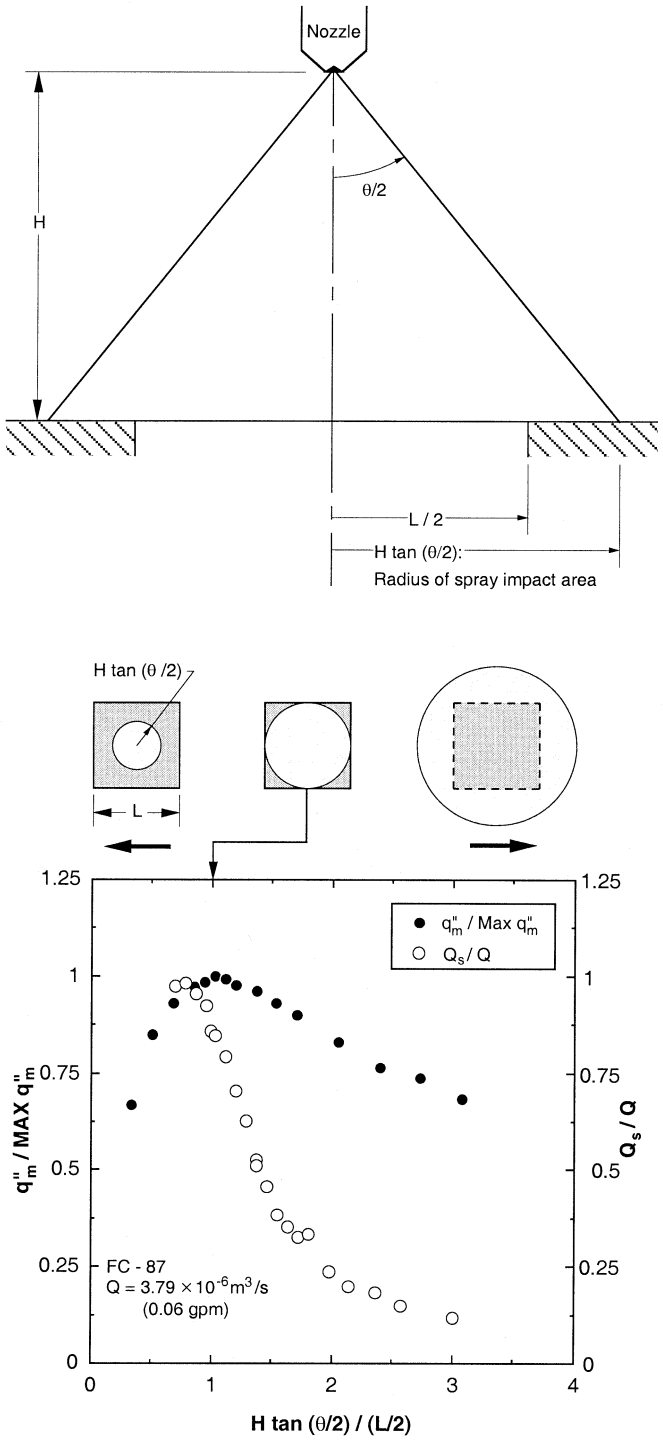

Fig. 24. Optimization of spray nozzle-to-wall distance to maximize CHF (adapted from [76]).

but not eliminate them altogether. As the inlet liquid velocity was increased, the CHF values showed a weaker dependence on orientation. Data for the highest velocity, (400 cm/s) and lowest subcooling (3°C) in Fig. 12 show very little change in CHF with orientation. The effect of orientation on CHF was negligible for inlet fluid velocities greater than 200 cm/s for near-saturated flow and 150 cm/s for highly subcooled flow. Below these velocities, upflow yielded higher CHF values as compared to downflow and horizontal flow with downward-facing chips.

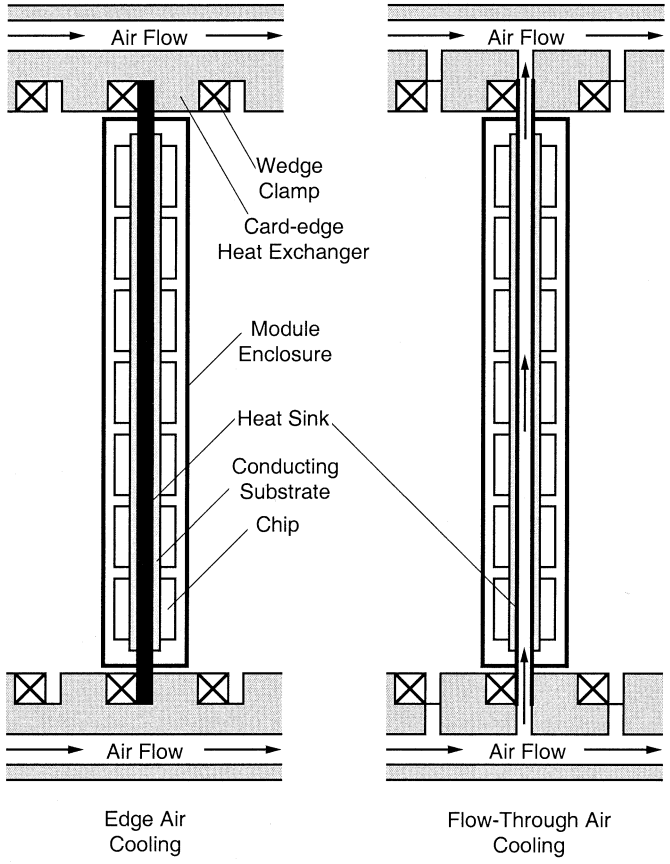

Fig. 25. Avionics air cooling schemes.

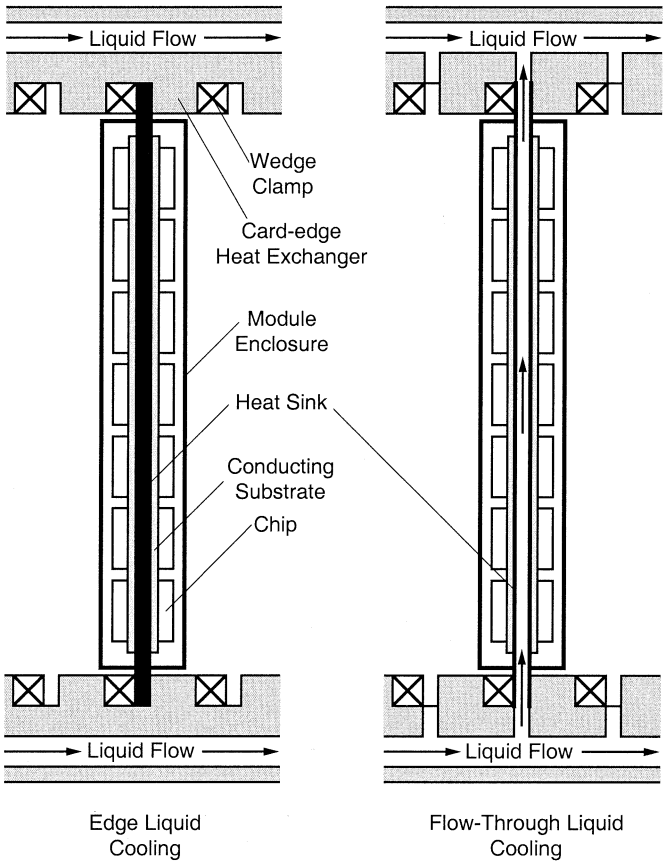

Fig. 26. Avionics indirect liquid cooling schemes.

The observations from these orientation studies are summarized in the polar diagram in Fig. 13. Just prior to CHF, the liquid and vapor flow characteristics in the channel and at the chip surfaces were postulated to fall into one of four categories:

a) local dryout of chip surface;
b) stratification of vapor above liquid;
c) vapor stagnation in the channel;
d) vapor counterflow causing liquid blockage.

Stratification occurred at low velocities for angles near $\theta = -90$ degrees while vapor counterflow was responsible for CHF for the rest of the downflow orientations. If lower downflow velocities were tested, perhaps flooding would have been observed to initiate CHF. For slightly higher velocities, CHF was a result of vapor stagnation. Critical heat flux for the rest of the downflow experiments and all of the upflow experiments was caused by localized dryout of the heater surface, proving high velocities may be the only means to completely dampen the effects of orientation on CHF. Overall, vertical upflow is the orientation of choice for packaging of multichip modules in two-phase cooling systems. This orientation insures consistent boiling, stable flow and high CHF.

Flow Curvature Effects: Stream-wise curvature has been shown to enhance both single- and two-phase heat transfer. Numerous applications involve heat transfer to a fluid flowing through a curved passage. For example, the coolant channels at the throat of a rocket engine, and the receiver coil of a solar power generation system both exhibit stream-wise curvature, with the additional characteristic of heating along a concave surface. Also, serpentine or spiral cooling passages with rectangular cross-sections can be milled or stamped into cold plates because of spatial limitations or purposely formed to capitalize upon the merits of curvature.

Many investigators have measured an enhancement in CHF along the concave surface of a flow channel compared to a straight channel with equal cross-sectional dimensions [43]–[45]. However, there is still some disagreement over the effects of centripetal acceleration on CHF enhancement. Gambill and Green [46] and Gu *et al.* [47] correlated their respective CHF enhancement factors with centripetal acceleration to the one-fourth power, drawing on the pool boiling correlation proposed by Zuber *et al.* [28] which contained earth's gravity to the 1/4-power.

Recently, Sturgis and Mudawar [48], [49] performed detailed photomicrographic studies of the vapor coalescence that results in the formation of a vapor layer along a concave surface at CHF. Fig. 14 shows a clear tendency of the centripetal force to pull vapor inward removing it from the concave wall, especially near the leading edge of the concave heater where the vapor is being elongated radially inward and pinched off. Farther downstream, vapor is removed from the concave wall, fragmented and distributed throughout the cooler bulk flow where it is better able to condense. In this way, curved flow is very effective at utilizing the available subcooling throughout the cross-section. This vapor coalescence behavior is in sharp contrast to straight channels where the vapor coalesces into a wavy vapor layer that is confined to the heated wall, impeding liquid access to the wall.

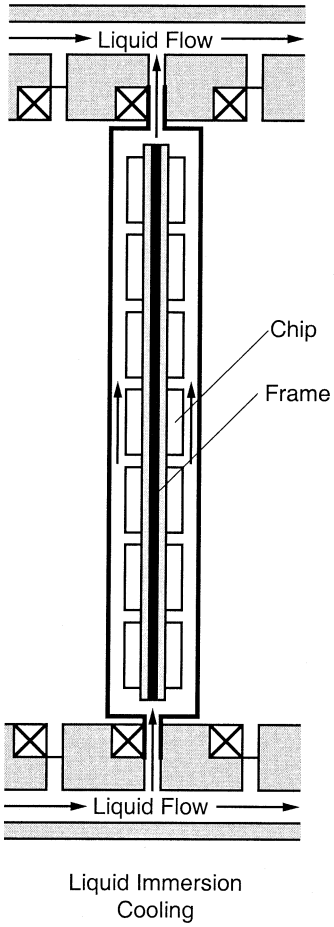

Fig. 27. Avionics liquid-immersion cooling scheme.

Also, the greater height of vapor patches near the inlet region in the curved channel are associated with a greater curvature of the vapor–liquid interface, which results in a larger pressure difference across the interface in regions of liquid contact with the concave wall. This pressure force acts to maintain liquid contact with the surface by more effectively resisting the momentum of vapor produced in the liquid contact regions, leading to an increased CHF.

Sturgis and Mudawar [48], [49] conducted tests corresponding to up to 315 earth g's. The curvature augmented CHF by about 60 percent for near-saturated flow and only 20 percent for highly subcooled flow. Clearly, the enhancement in CHF is better realized at low subcooling where a larger vapor volume is produced and because the flow is more dependent upon the centripetal force for vapor removal. These studies disputed the analogy with the Zuber *et al*. CHF model for pool boiling since CHF enhancement relative to straight channels was far smaller than the centripetal acceleration to the one-fourth power.

C. Microchannel and Minichannel Cooling

Merits of Two-Phase Microchannel and Minichannel Cooling: The term "micro" is loosely applied to modern cooling devices having hydraulic diameters of ten to several hundred micrometers [50], [51], while "mini"-channels refers to diameters on the order of one to a few millimeters [51]–[53]. The small flow rate within micro-channels produces laminar flow which, in the absence of phase change, results in a heat transfer coefficient inversely proportional to the hydraulic diameter. While enormous single-phase heat transfer coefficients are possible simply by decreasing the hydraulic diameter, very large pressure drops accompany the dissipation of high heat fluxes. Furthermore, single-phase microchannel heat sinks compensate for high heat fluxes by a large stream-wise increase in the coolant temperature and a corresponding stream-wise increase in the temperature of the heat dissipating device. This increase is often very detrimental to temperature-sensitive devices such as electronic chips.

Two-phase micro-channel cooling, on the other hand, permits partial or total consumption of liquid by evaporation, thus requiring minimal coolant flow rates. Two-phase heat sinks also rely upon latent heat exchange that helps maintain stream-wise temperature uniformity, both in the coolant and the heat sink, to a level that is largely dictated by the coolant saturation temperature.

Microchannel and Minichannel Cooling Configurations: There are two main configurations for adaptation of micro- and mini-channel two-phase cooling. These are direct cooling and indirect cooling. As shown in Fig. 15(a), direct cooling involves immersion of the device surface directly in the liquid coolant. This scheme shortens the thermal resistance between the surface and the coolant, enabling the dissipation of large heat fluxes at relatively low surface temperatures. The main drawback of this system is the need to ensure electrical and chemical compatibility between the device itself and the coolant. An example of this direct cooling configuration is the avionics cooling module developed Jimenez and Mudawar [54].

Fig. 15(b) shows an alternative cooling scheme involving the use of a metallic heat sink to conduct the heat away from the device to a coolant which is pumped inside circular or rectangular grooves in the heat sink. This scheme provides greater flexibility in the coolant selection. However, indirect cooling also increases the thermal resistance between the surface and the heat sink due to the heat diffusion resistance in the heat sink itself. The heat sink with the rectangular grooves is becoming the cooling method of choice for many high-flux and ultra-high-flux devices because these grooves can be milled using a number of conventional and microfabrication methods. While the later methods can produce micron-sized features, studies (with single-phase coolants) point to a practical minimum hydraulic diameter of about 200 μm below which the likelihood of clogging increases very drastically [55].

But by far the most severe limitation to the use of microchannel heat sinks is critical heat flux (CHF). Since the cooling requirements in high-flux and ultra-high-flux devices exceed the critical heat flux attainable with common flow boiling configurations, the ability to both greatly increase and predict the magnitude of CHF is of paramount importance to the development of these devices.

CHF in Microchannel and Minichannel Flow: Many other terms are used interchangeably in the heat transfer literature to describe CHF. "Departure from nucleate boiling" (DNB) is often used to describe the process of vapor film (blanket) formation at the heated wall in predominantly high mass velocity

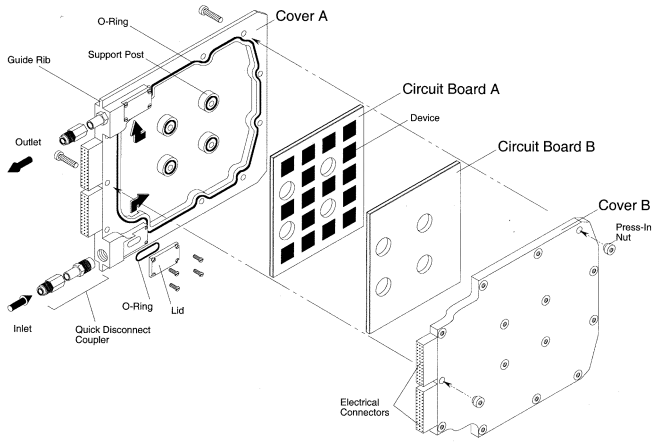

Fig. 28. Construction of BTPFL-C1 clamshell module (adapted from [81]).

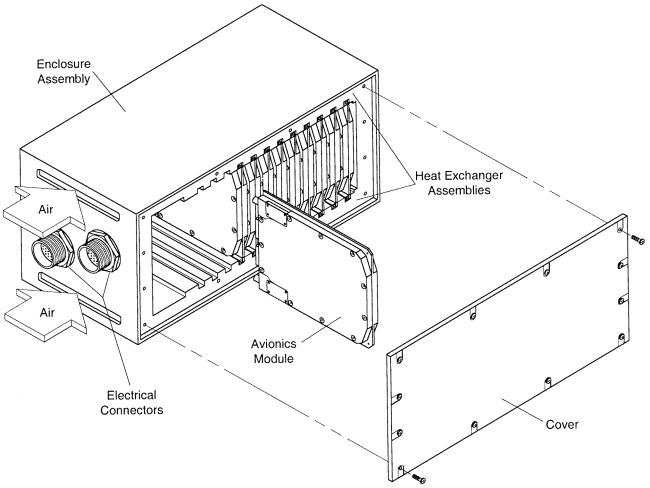

Fig. 29. Standard avionics enclosure.

(product of liquid density and liquid inlet velocity) and highly subcooled flows. "Dryout", on the other hand, is used to denote liquid film dryout in annular flow corresponding to low mass velocity and low subcooling flows. Below are brief descriptions of the dryout and the burnout regimes of CHF in micro-channel flow.

Dryout CHF Regime: Low and high mass velocity flows are characterized by drastically different flow patterns as well as unique CHF trigger mechanisms. Shown on the left-hand side of Fig. 16 is a liquid entering a uniformly heated tube at low velocity. The combination of low mass velocity, low subcooling and a long tube often results in a near saturated vapor flow at the tube exit. Boiling occurs downstream from the inlet as the flow pattern develops from bubbly to slug and/or churn-turbulent, followed by annular. The boiling subsides when the liquid film in the annular regime becomes too thin to sustain bubble nucleation and forced convection heat transfer to the film, along with interfacial evaporation, ensue. Eventually, the film dries out due to complete liquid evaporation. Liquid film dryout is the mechanism responsible for the relatively low CHF values associated with saturated boiling in long tubes with low inlet subcooling. But even with film dryout, an appreciable amount of liquid may still be present at the exit in the form of droplets entrained in the vapor flow.

Bowers and Mudawar [51]–[53] examined this form of CHF for high-flux electronic cooling. As shown in Fig. 17, micro- and mini-channel heat sinks were heated by a thick-film resistor that simulated an electronic device. The heat sink was press fit into a fiberglass plastic housing. CHF values well in excess of 100 W/cm^2 were obtained using R-113 as coolant at extremely low flow rates (up to a maximum of 95 ml/min). One unique feature of these heat sinks was the ability to evaporate all of the coolant before CHF was detected. This form of dryout CHF has never been observed before. It is believed the small diameter of the heat sink channel enhances droplet impact with the channel walls which, along with the heat sink's ability to conduct heat away toward the channel inlet, helps evaporate all of the liquid droplets. The superheated exit conditions measured in these heat sinks before CHF is evidence that, unlike most boiling systems, cooling with miniature heat sinks is possible with an evaporation efficiency of unity (i.e., minimal coolant flow rate).

A comparison of boiling curves for two channel sizes is shown in Fig. 18(a). The curves are characterized by a distinct offset in the single-phase region with the smaller channel exhibiting superior heat transfer performance; however, within the nucleate boiling regime, the distinction is less discernible. Approaching CHF, the heat transfer coefficient drops off more with the larger than with the smaller, before reaching a maximum heat flux of 200 W/cm^2 as compared to 256 W/cm^2 for the smaller channel. The smaller channel yielded this 28 percent increase in CHF at the expense of a larger pressure drop as shown in Fig. 18(b). Within the single-phase region, pressure drop for both heat sinks is low ($\Delta P < 0.02$ bar); however, there is a large difference in pressure drop in the boiling region. This is especially true for higher fluxes above 100 W/cm^2, where pressure drop for the smaller channel climbs to values in excess of 0.30 bar while the larger channel pressure drop remains below 0.03 bar. A detailed pressure drop model of each heat sink proved the major contributor to pressure drop is the acceleration resulting from evaporation. Furthermore, compressibility effects are far more significant for the micro-channel. Large pressure drop and the potential for choking warrant the use of channel diameters no smaller than the micro-channel ($D = 510$ μm) for high flux applications.

DNB Regime: High mass flow in a short tube with high inlet subcooling results in subcooled boiling and higher CHF values as illustrated by the tube on the right-hand side of Fig. 16. In this case, very small bubbles are formed creating a thin bubble boundary layer, and bubbles migrating toward the core quickly condense. The core temperature rises as a result of the energy transfer; however, the flow remains in the subcooled boiling region over its entire heated length. CHF can occur while the core liquid is well below the saturation temperature and is commonly referred to as departure from nucleate boiling (DNB). For high-flux DNB, the term "burnout" heat flux is also used because physical destruction of the system will occur as a result of a large surface temperature excursion.

The above classification points to key parameters affecting flow boiling CHF for any cooling configuration. These are mass velocity, subcooling, pressure, hydraulic diameter, heated

length, and, of course, the coolant itself. Previous studies provide ample evidence ultra-high-fluxes are possible with highly subcooled flow boiling of water at high mass velocity in micro-channels [56]–[60].

Recent studies at Purdue University have confirmed ultra-high CHF values in excess of 10^4 W/cm^2 can be achieved with subcooled water flow at high velocities in small diameter tubes ($D < 1$ mm) of short heated lengths ($L < 6$ mm). These experiments yielded the highest recorded CHF value for a uniformly heated tube of $27{,}600$ W/cm^2 [61], [62]. Fig. 19 shows a photograph of the test section following burnout at this ultra-high heat flux.

D. Jet-Impingement Cooling

Jet-impingement is typically used in applications demanding the dissipation of both transient and steady concentrated heat loads. For example, jet-impingement is widely used to quench metal alloy parts from very high temperatures in order to achieve a desired alloy microstructure and superior mechanical properties. Jet-impingement has also been widely used to maintain relatively low, steady temperatures in devices which dissipate enormous heat fluxes such as lasers and x-ray anodes. Jet-impingement can be implemented in three basic forms: free jet (liquid jet issued in a vapor or gaseous ambient), submerged jet (liquid jet formed in a liquid ambient) and confined jet (liquid jet confined between the nozzle and heated wall). Jets can be issued from a circular or a rectangular orifice. Since jets concentrate most of the cooling directly within the impact zone, multiple jets are also commonly used to diffuse this cooling concentration by creating several high-heat-flux impingement regions. In all these forms, jet-impingement is considered an aggressive form of cooling due the large impact momentum upon the heated surface, which may not be allowable with delicate devices.

Several investigators examined the two-phase cooling characteristics of free circular jets. In the absence of boiling, a free jet forms a radial wall jet that emanates from the impingement zone while remaining mostly in contact with the heated wall. During boiling, however, the vigorous effusion of vapor within the wall jet begins to splash away a significant portion of the wall jet liquid flow [63]–[66]. Further increases in heat flux result in the formation of dry patches in the outer circumference of the wall jet as much of the wall jet liquid is splashed away in these outer regions. Eventually, this dryout propagates inwards toward the impingement zone, causing separation of the wall jet from much of the heated wall and resulting in CHF as illustrated in Fig. 20. Estes and Mudawar [67] showed CHF for free circular jets can be enhanced by increasing jet velocity, Fig. 21, or jet diameter. But increasing subcooling was especially beneficial in condensing the vapor bubbles in the radial wall jet, thus greatly delaying the wall jet separation caused by the bubble growth.

In order to investigate rectangular jet-impingement heat transfer at both the chip and module levels, Mudawar and Wadsworth [68] developed a muti-chip cooling module that was capable of uniformly supplying coolant to, and rejecting it from each chip. Fluorinert FC-72 was supplied independently to each chip in a 3×3 array of 12.7×12.7 mm^2 chips via a single rectangular slot facing each chip. CHF was measured

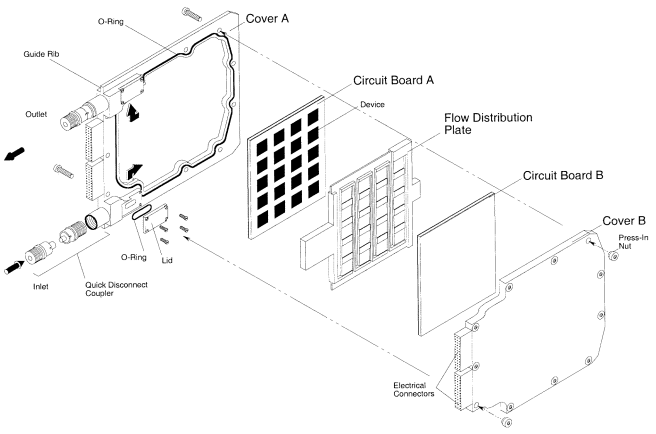

Fig. 30. Construction of BTPFL-C2 clamshell module (adapted from [54]).

for broad ranges of jet width, jet height, jet velocity, and fluid subcooling. Velocity had a pronounced influence on all regions of the boiling curve. An enhancement of over 300 percent in CHF was achieved when impingement velocity was increased from 1 to 11 m/s. Dramatic CHF enhancement was also achieved by increasing the subcooling of the liquid. Perhaps the most important practical conclusion from their study is that jet velocity has a stronger effect on CHF than jet width. This means for a fixed coolant flow rate CHF can be increased by increasing the jet velocity. Therefore, the coolant flow rate requirements for rectangular jets can be reduced simply by choosing a smaller jet width.

E. Spray Cooling

Like jet-impingement, spray cooling has long been employed in the quenching of metals. Unfortunately, most spray quenching studies concern high temperatures corresponding to the film boiling regime [69]–[71] and are not applicable to electronic cooling. Several studies have been published during the last three decades which address the lower temperature nucleate boiling regime of spray cooling [72]–[74]; some of the more recent ones are directly related to electronic cooling [67], [75]–[77].

Sprays can be classified into either pressure sprays or atomized sprays, depending upon the method used to accomplish the liquid breakup. Pressure sprays are formed by supplying liquid at high pressure through a small orifice while atomized sprays employ a high-pressure air stream to assist the liquid breakup. Despite their superior cooling performance, atomized sprays are difficult to incorporate in a closed loop electronic cooling system because of the complexity of separating air (or inert gas) from dielectric liquid coolants.

Spray and free-jet cooling are often considered competing options for electronic cooling. For the most part, sprays reduce flow rate requirements but require a higher nozzle pressure drop. As indicated in the previous section, one disadvantage of jet-impingement cooling is the concentration of heat removal within the impingement zone causes relatively large temperature gradients within the cooled device. Jet-impingement cooling is also prone to separation of the wall liquid layer emanating from the impingement zone during vigorous boiling. Sprays, on the other

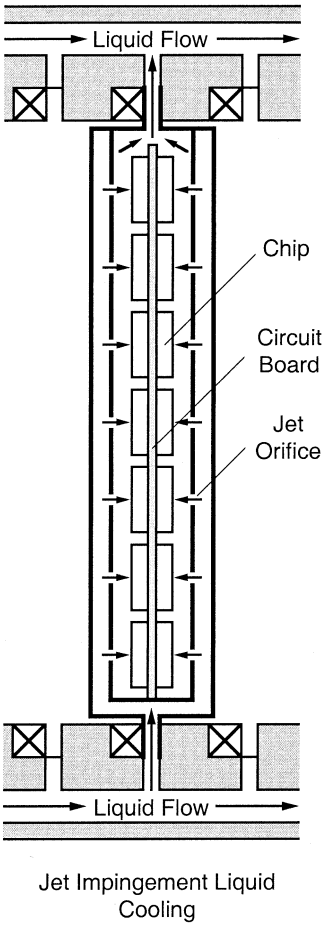

Fig. 31. Avionics two-phase jet-impingement cooling module.

hand, break up the liquid into fine droplets which impinge individually upon the heated wall. The droplet impingement both enhances the spatial uniformity of heat removal, Fig. 22, and delays the liquid separation from the wall during vigorous boiling.

Despite these advantages, sprays have not gained popularity in electronic cooling because the intricate flow features within spray nozzle increase the likelihood of clogging. Furthermore, spray nozzles require careful periodic testing to ensure predictable and repeatable impact pattern. Even seemingly identical nozzles from the same production batch often fail to produce identical spray patterns [78].

The author and co-workers recently explored several aspects of nucleate boiling and CHF in pressure sprays. Initial efforts revealed the cooling characteristics of sprays are sensitive mostly to the spray volumetric flux, Q'', and Sauter mean diameter, d_{32} [73], [74], [78]. Q'' is defined as the volume flow rate of liquid impacting an infinitesimal portion of the impact area divided by the area of the same portion.

More recently, Estes and Mudawar [67], [75], [76] investigated spray boiling and CHF from a square heater that simulated an electronic device. Boiling curves were measured for different nozzles over broad ranges of flow rate and subcooling. Shown in Fig. 23 are FC-72 boiling curves for three flow rates. These boiling curves show only a minute increase in slope at incipient boiling. This demonstrates another key drawback to spray cooling: the low wall temperature merit of nucleate boiling (which is common to jets and other flow boiling systems) is not always realized with sprays.

Unlike jets, sprays produce drastically different cooling performances for the same nozzle and same flow rate depending upon the nozzle-to-surface distance. Therefore, this distance should be carefully selected to ensure both repeatability and predictability of cooling performance, especially near CHF. Mudawar and Estes [76] optimized CHF by examining the effect of nozzle-to-surface distance on both CHF and corresponding fraction of the spray liquid which impacts the heated surface. As illustrated in Fig. 24, with a small nozzle-to-surface distance, only a small fraction of the heater surface is directly impacted by the spray and the corresponding CHF is relatively small. Small CHF values are also encountered when the nozzle-to-surface distance is too large because a fraction of the spray liquid would fail to impact the heater surface. CHF is a maximum when the spray impact area just inscribes the square surface of the heater. Thus, the appropriate nozzle-to-surface distance can be easily determined knowing only the size of the heater and the spray angle. Higher CHF values were also achieved by increasing the total spray flow rate and the liquid subcooling at the nozzle inlet. The same study provides a comprehensive methodology for determining the magnitude of the optimum CHF, the Sauter mean diameter, and the spatial distribution of volumetric flux.

III. Thermal Management of Avionics

A. Background

Thermal management is a primary design concern for both military and commercial avionics. The U.S. Department of Defense has been at the forefront in developing techniques and standardized hardware for high-performance avionics (e.g., the Standard Electronic Module (SEM) program [54]). To meet the increasing heat dissipation challenges, efforts such as the Air Force Pave program were initiated to develop new standard modular avionics for future aircraft.

Thermal management in most of today's military Standard Electronic Module-format E (SEM-E) modules consists of conducting the heat away from the device through a thermal network consisting of a solder layer, a multilayer circuit board, card rails and a compact heat exchanger. This heat exchanger rejects the heat to the aircraft-supplied cooling air as illustrated in Fig. 25. The relatively large thermal resistance associated with edge air cooling limits the use of this cooling scheme to avionics modules dissipating no more than 40 W. While some improvement in cooling performance is possible by supplying the air through the module itself, Fig. 25, air cooling schemes are no longer capable of meeting demands of high performance avionics modules. Recent studies have shown some of the advanced avionics are experiencing nearly an order-of-magnitude increase (up to 200 to 300 W for SEM-E modules) in power/cooling requirements [79].

The drastic increase in the cooling requirements of advanced avionics has lead to the introduction of liquid cooling schemes which capitalize upon the superior thermal transport properties of liquid coolants and the merits of phase change. Like air

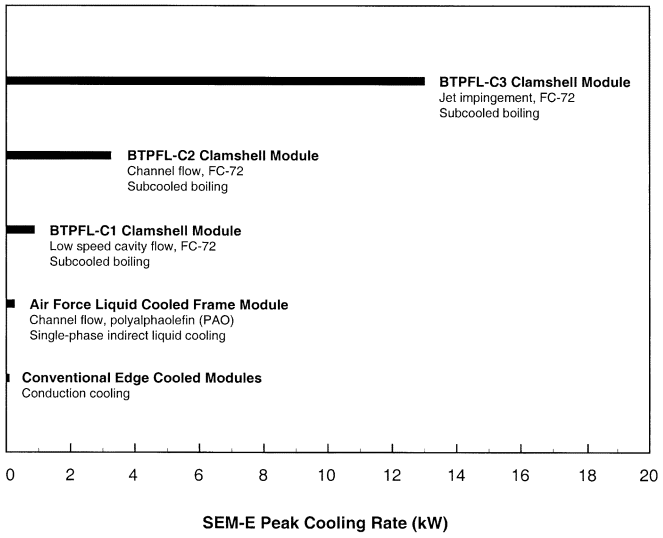

Fig. 32. Comparison of performances of different avionics cooling modules.

cooling, liquid cooling can also be achieved along the edge of the board or through the SEM-E module itself, Fig. 26. Far superior results are possible when the liquid coolant is brought in direct contact with the device itself, Fig. 27.

The Air Force Pave program culminated in the development of a new building block for high performance avionics that is compatible with conventional SEM-E circuit boards and connector requirements [80]. Using the flow-through liquid cooling scheme illustrated in Fig. 26, polyalphaolefin (PAO) liquid was circulated through a hollow, vacuum-brazed aluminum frame onto which the devices were bonded. This cooling module featured a sleeveless, drip-free quick connection liquid couplers with an outer envelope smaller than 1.5 cm (0.6 in). While further improvements in the thermal performance of this flow-through module are underway, studies point to an upper cooling rate of 250 W. This limit is largely due to limitations on the single-phase convective heat transfer coefficient of PAO, the thermal resistance between the device and coolant, and the enormous pressure drop associated with high PAO viscosity at sub-zero ambient temperatures.

The performance of PAO flow-through modules marks a threshold for single-phase liquid cooling in avionics. New thermal management schemes have had to be continually developed or existing ones updated to barely keep up with cooling needs. What has been lacking, thus far, are schemes with far superior cooling potential that could accommodate the large increases in cooling requirements anticipated for the coming decade.

B. Phase Change Avionics Cooling

Recognizing the merits of subcooled immersion cooling with phase change, the U.S. Navy established a program at Purdue University that was aimed at replacing the PAO flow-through module with an immersion cooling "clamshell" module, the BTPFL-C1, of identical outer envelope (1.5 cm thickness), which is compatible with existing avionics enclosure packaging constraints [81]. The initial goal of this program was to dissipate 500 W from two circuit boards that were submerged in dielectric FC-72 inside the module cavity. Phase change was key to achieving this superior performance. Fig. 28 shows an exploded view of the BTPFL-C1 clamshell module.

Fig. 29 shows how such BTPFL-C1 clamshell modules can be mounted side by side in a conventional avionics enclosure. The modules are secured by wedge clamps that ensure both fluid and electrical coupling of the clamshell module with mating hardware in the enclosure backboard. An FC-72 pump and accumulator are located either within the enclosure itself or in an external housing. When employed with a conventional air cycle environmental control system (ECS), heat is rejected from the module fluid to the aircraft compressed air via heat exchanger assemblies located in the top and bottom walls of the enclosure.

Several stringent requirements were imposed on the design of the BTPFL-C1, which included, aside from the SEM-E outer envelope and the 500 W heat dissipation, minimizing coolant flow rate and pressure drop, maintain device temperatures below 125°C, and limiting coolant interfacing to two sleeveless, drip-free quick connection couplers having an outer envelope no greater than the total module thickness. Another important design requirement was to condense all of the vapor produced in the module cavity prior to exiting the module, thus simplifying the coolant conditioning by employing an essentially single-phase flow loop external to the module.

To further enhance the thermal performance of the BTPFL-C1, designs other than an open cavity must be considered. Previous electronic cooling studies have revealed that critical heat flux (CHF) can be greatly increased by (a) using enhanced surface features which are formed directly upon each device and (b) increasing the coolant velocity. Size, complexity and weight constraints render surface enhancement less attractive for avionics. Enhancing cooling performance therefore requires increasing coolant velocity. Increasing the coolant velocity can be accomplished even with a small flow rate by reducing the flow area adjacent to the chip surface, i.e., using micro- or mini-channel flow. Jimenez and Mudawar [54] explored the effectiveness of using narrow channels by developing a new module, the BTPFL-C2, which is illustrated in Fig. 30. The outer clamshell of the BTPFL-C2 is identical to that of the BTPFL-C1, the primary difference between the two modules is the use of a flow distribution plate between the circuit boards of the BTPFL-C2. This plate creates a number of parallel micro- or mini-channels between the flow distribution plate itself and the device surface; coolant flow is undirected inside the cavity of the BTPFL-C1. The unique attributes of micro- and mini-channel cooling enabled the BTPFL-C2 to dissipate in excess of 3000 W, one order of magnitude greater than the Pave PAO flow-through module. Device heat fluxes as high as 44 W/cm^2 were achieved with the BTPFL-C2 compared to 16 W/cm^2 with the BTPFL-C1.

Another advancement in the development of phase-change immersion cooled modules is the development of the BTPFL-C3 module [82]. This module is double-pitched, meaning it is twice the thickness of the BTPFL-C1 and BTPFL-C2, ensuring electrical and fluid connection compatibility with SEM-E avionics enclosures. As shown in Fig. 31, the BTPFL-C3 employs direct jet-impingement of FC-72 upon the device surface using a single or multiple circular

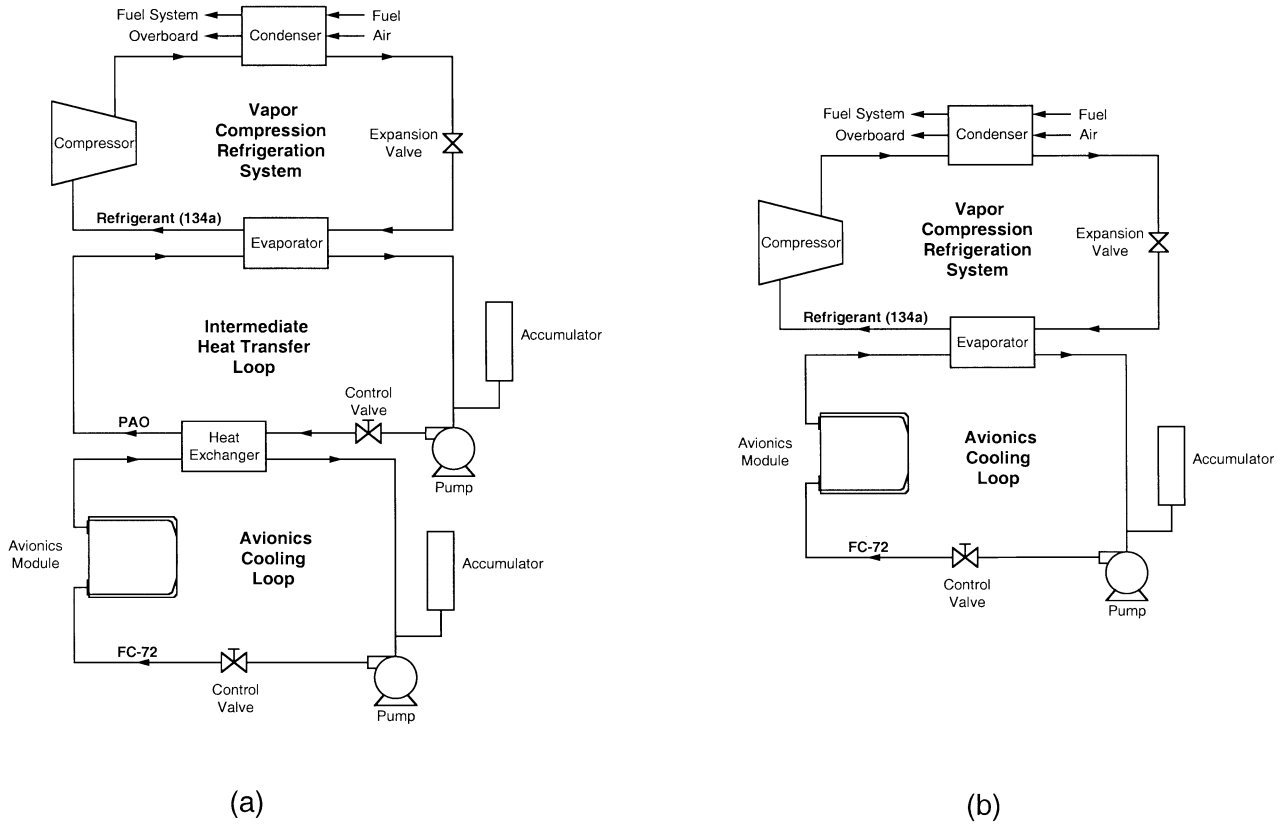

Fig. 33. Interfacing of two-phase avionics cooling loop with vapor compression refrigeration system (a) via PAO intermediate cooling loop and (b) without an intermediate loop.

jets that are confined between the flow distribution plate and device surface. The BTPFL-C3 performance exceeded 10 kW, eclipsing the performance of the Pave PAO flow-through module by two orders of magnitude. Device heat fluxes as high as 255 W/cm^2 were possible with the BTPFL-C3. Fig. 32 compares the performance of the PAO flow-through module to those of the BTPFL-C1, BTPFL-C2, and BTPFL-C3.

The enormous enhancement in cooling performance demonstrated with each of the three clamshell modules was accomplished by applying lessons learned from several of the fundamental studies discussed earlier in this paper. Namely, as follows.

a) Replacing air cooling and indirect liquid cooling with direct-immersion cooling.
b) Capitalizing upon the merits of phase change.
c) Enhancing the cooling performance through better liquid access to the surface using such configurations as micro- and mini-channel flow and confined jet impingement.
d) Greatly increasing the coolant subcooling at the module inlet to

   1) reduce vapor production within the module;
   2) increase CHF;
   3) condense bubbles before they exit the module.

   Bubble condensation has the benefits of both simplifying coolant conditioning external to the module, by employing essentially a single-phase liquid loop, and reducing coolant flow sensitivity to the large body forces encountered in military aircraft.

C. Practical System Considerations

Ironically, the clamshell program also demonstrated that practical systems considerations play a paramount role in determining cooling performance. One of the key limitations was determined to be the fluid couplers used to supply the coolant into and from the module! These couplers contain several internal seals designed to prevent air inclusion or coolant spillage during the insertion (or removal) of clamshell module into (out of) the avionics enclosure. Intricate mating surfaces to preclude misalignment between the coupler's mating parts are also required. The delicate design of the couplers, and the small outer envelope (less than 1.5 cm), place an upper limit on coolant flow rate of about 3.2×10^{-5} m^3/s (0.5 gpm) for single-pitch clamshell modules. It is possible to greatly increase this flow rate limit by utilizing a dual pitch module that would still conform to the packaging constraints of standard avionics enclosures. A dual pitch module would provide room for both larger diameter couplers and thicker module walls. Since coolant pressure drop is proportional to flow passage diameter to the negative fourth power, doubling the outer envelope of the couplers allows a 16-fold increase in the coolant flow rate for the same pressure drop. With the additional wall strength

and corresponding increase in allowable pressure drop with a dual pitch module, it is possible to increase the flow capacity of the module to about 9.5×10^{-4} m^3/s (15 gpm), thus greatly increasing the cooling capacity relative to a single pitch module.

Another important practical consideration in the implementation of the clamshell modules is the interfacing of the coolant conditioning loop with the aircraft environmental control system (ECS). Two possible heat sinks for the conditioning loop are the aircraft air and fuel. Air provided by the aircraft through bleed air from the engine and by ram air scoops, and the spent air is ejected into the environment. Using fuel as a heat sink has advantages but also limitations. The key advantages are reduction in heat exchanger size and weight compared to a coolant-to-air heat exchanger, reduction in the amount of bleed air required to cool the avionics (thus minimizing engine performance penalties), and elimination of dependence on ram air scoops. The limitations in using fuel as a heat sink are fuel volatility, limited thermal mass and maximum permissible fuel temperature.

Integration of an avionics subsystem into an existing environmental control system requires assessment of its impact on the cooling of other aircraft subsystems. Typically, an intermediate heat transport loop is plumbed to all electronic heat loads throughout the aircraft. This loop serves to transport the thermal energy to the air or fuel. The system currently preferred on military aircraft consists of a an intermediate heat transport loop utilizing polyalphaolefin (PAO). In some cases, a vapor compression refrigeration system dissipates the heat from the PAO heat transport loop to the aircraft fuel system.

Two interfacing options are possible for high performance immersion-cooled clamshell modules. The first, Fig. 33(a), consists of rejecting the heat from the FC-72 loop's heat exchanger to polyalphaolefin (PAO) which flows through a general utility loop similar to the one presently recommended for military aircraft. The heat is then rejected from the PAO to the vapor compression refrigeration system that, in turn, rejects its heat to aircraft fuel via a condenser. Fig. 33(b) shows the second interfacing option which consists of eliminating the PAO loop altogether and rejecting the heat from the avionics cooling loop directly to the vapor compression refrigeration system.

While these two options may point to great flexibility in the implementation of immersion cooling, great care should to be exercised when integrating the FC-72 cooling loop alongside other aircraft subsystems that require heat removal. Subsystem heat loads can be managed in series or in parallel. A parallel arrangement may be difficult to implement given the flow rate limitations of the vapor compression refrigeration system or PAO general utility loop. If subsystems are managed in series, a hierarchy must be developed based on the cooling needs and temperature requirements of the different subsystems. The refrigerant in the vapor compression refrigeration system or PAO in the general utility loop would pass through the various systems sequentially, starting with the subsystem requiring the lowest inlet temperature. Such a hierarchy may preclude situating the FC-72 heat exchanger at the optimum location, negating some of the advantages of a highly subcooled FC-72 module inlet condition.

IV. Conclusion

Many cooling schemes have been investigated and developed which are capable of dissipating the high heat fluxes presently encountered or projected for high performance electronic devices. This paper explored the important thermal and practical attributes of individual schemes. Key findings from this study are as follows.

1) Each of the cooling schemes discussed in this paper (pool boiling, detachable heat sinks, channel flow boiling, micro-channel and mini-channel heat sinks, jet-impingement, and sprays) is capable of dissipating over 100 W/cm^2 using dielectric coolants known to possess relatively poor thermal transport properties.
2) Phase change plays a key role in attaining these attractive cooling performances. However, phase change systems are generally more complicated to implement than single-phase liquid-cooled systems. The primary concern with phase change cooling is the ability to predict CHF in order to ascertain a comfortable factor of safety relative to device heat dissipation. Many methods exist for enhancing CHF, especially surface enhancement, high coolant velocity and subcooling.
3) Selecting a suitable cooling system for a particular application involves several important criteria such as heat dissipation potential, reliability, and packaging concerns. While the different cooling schemes discussed in this paper can be tailored to the specific needs of individual applications, system considerations always play a paramount role in determining the most suitable cooling scheme.
4) Extensive fundamental heat transfer knowledge that is directly associated with electronic cooling has been amassed over the past two decades. Yet, there is now a growing need for hardware innovations rather than perturbations to these fundamental studies. Such innovations will require close collaboration between research teams from both industry and academe.

References

[1] R. D. Boyd, "Subcooled flow boiling critical heat flux (CHF) and its application to fusion energy components—Part I. A review of fundamentals of CHF and related data Bbase," *Fusion Tech.*, vol. 7, pp. 7–31, 1985.

[2] C. S. Rogers, D. M. Mills, W. K. Lee, G. S. Knapp, J. Holmberg, A. Freund, M. Wulff, M. Rossat, M. Hanfland, and H. Yamaoka, "Performance of a liquid-nitrogen-cooled, thin silicon crystal monochromator on a high-power, focussed wiggler synchrotron beam," *Rev. Sci. Instrum.*, vol. 66, pp. 3494–3499, 1995.

[3] T. M. Anderson and I. Mudawar, "Microelectronic cooling by enhanced pool boiling of a dielectric fluorocarbon liquid," *ASME J. Heat Transf.*, vol. 111, pp. 752–759, 1989.

[4] I. Mudawar, "Direct-immersion cooling for high power electronic chips," in *Proc. I-Therm III: Intersoc. Conf. Thermal Phenom. Electron. Syst.*, Austin, TX, Feb. 3–5, 1992, pp. 74–84.

[5] I. Mudawar and T. M. Anderson, "Parametric investigation into the effects of pressure, subcooling, surface augmentation and choice of coolant on pool boiling in the design of cooling systems for high-power density chips," *ASME J. Electron. Packag.*, vol. 112, pp. 375–382, 1990.

[6] M. D. Reeber and R. G. Frieser, "Heat transfer of modified silicon surfaces," *IEEE Trans. Comp., Hybrids, Manufact. Technol.*, vol. CHMT-3, pp. 387–391, Sept. 1980.

[7] R. L. Webb, "The evolution of enhanced surface geometries for nucleate boiling," *Heat Transf. Eng.*, vol. 2, pp. 46–69, 1981.

[8] A. E. Bergles and M. C. Chyu, "Characteristics of nucleate boiling from porous metallic coatings," *ASME J. Heat Transf.*, vol. 104, pp. 279–285, 1982.

[9] P. J. Marto and V. J. Lepere, "Pool boiling heat transfer from enhanced surfaces to dielectric fluids," *ASME J. Heat Transf.*, vol. 104, pp. 292–299, 1982.

[10] W. J. Miller, "Boiling and visualization from microconfigured surfaces," M.S. thesis, Univ. Pennsylvania, Philadelphia, PA, 1991.

[11] S. H. Bhavnani, C. P. Tsai, R. C. Jaeger, and D. L. Eison, "An integral heat sink for cooling microelectronic components," *ASME J. Electron. Packag.*, vol. 115, pp. 284–291, 1993.

[12] S. S. Murthy, Y. K. Joshi, and W. Nakayama, "Single chamber compact thermosyphons with micro-fabricated components," in *Proc. Itherm'00*, vol. 2, Las Vegas, NV, May 23–26, 2000, pp. 321–327.

[13] A. D. Messina and E. L. Park, "Effects of precise arrays of pits on nucleate boiling," *Int. J. Heat Mass Transfer*, vol. 24, pp. 141–145, 1981.

[14] K. A. Park and A. E. Bergles, "Boiling heat transfer characteristics of simulated microelectronic chips with detachable heat sinks," in *Proc. 8th Int. Heat Transf. Conf.*, vol. 4, San Francisco, CA, 1986, pp. 2099–2104.

[15] W. Nakayama, T. Nakajimi, and S. Hirasawa, "Heat sink studs having enhanced boiling surfaces for cooling of microelectronic components," in *Proc. ASME Conf.*, 1984.

[16] I. Mudawar and T. M. Anderson, "Optimization of extended surfaces for high flux chip cooling by pool boiling," *ASME J. Electron. Packag.*, vol. 115, pp. 89–100, 1993.

[17] G. F. Goth, M. L. Zumbrunnen, and K. P. Moran, "Dual-tapered piston (DTP) module cooling for IBM enterprise system/9000 systems," *IBM J. Res. Develop.*, vol. 36, pp. 805–816, 1992.

[18] S. J. Reed and I. Mudawar, "Enhancement of boiling heat transfer using highly wetting liquids with pressed-on fins at low contact forces," *Int. J. Heat Mass Transf.*, vol. 40, pp. 2379–2392, 1997.

[19] S. Ishigai, K. Inoue, Z. Kiwakik, and T. Inai, "Boiling heat transfer from a flat surface facing downward," in *Proc. 1961–1962 Int. Heat Transf. Conf.*, Boulder, CO, 1961, pp. 224–229.

[20] P. M. Githinji and R. H. Sebersky, "Some effects of the orientation of the heating surface in nucleate boiling," *ASME J. Heat Transf.*, vol. 85, p. 379, 1963.

[21] R. P. Anderson and L. Bova, "The role of downfacing burnout in post-accident heat removal," *Trans. Amer. Nucl. Soc.*, vol. 14, p. 294, 1971.

[22] I. P. Vishnev, "Effect of orienting the hot surface with respect to the gravitational field on the critical nucleate boiling of a liquid," *J. Eng. Phys.*, vol. 24, pp. 43–48, 1974.

[23] M. S. El-Genk and A. Guo, "Transient boiling from inclined and downward-facing surfaces in a saturated pool," *Int. J. Refrigeration*, vol. 6, pp. 414–422, 1993.

[24] J. Y. Chang and S. M. You, "Heater orientation effects on pool boiling of micro-porous-enhanced surfaces in saturated FC-72," *ASME J. Heat Transf.*, vol. 118, pp. 937–943, 1996.

[25] T. Y. Chu, B. L. Bainbridge, R. B. Simpson, and J. H. Bentz, "Ex-vessel boiling experiments: laboratory and reactor scale testing of the flooded cavity concept for in-vessel core retention—Part I: Observations of quenching of downward-facing surfaces," *Nucl. Eng. Design*, vol. 169, pp. 77–88, 1997.

[26] I. Mudawar, A. H. Howard, and C. O. Gersey, "An analytical model for near-saturated pool boiling chf on vertical surfaces," *Int. J. Heat Mass Transf.*, vol. 40, pp. 2327–2339, 1997.

[27] A. H. Howard and I. Mudawar, "Orientation effects on pool boiling CHF and modeling of CHF for near-vertical surfaces," *Int. J. Heat Mass Transf.*, vol. 42, pp. 1665–1688, 1999.

[28] N. Zuber, M. Tribus, and J. M. Westwater, "The hydrodynamic crisis in pool boiling of saturated and subcooled liquids," in *Proc. 1961–62 Int. Heat Transf. Conf.*, Boulder, CO, 1961, pp. 230–236.

[29] D. E. Maddox and I. Mudawar, "Single and two-phase convective heat transfer from smooth and enhanced microelectronic heat sources in a rectangular channel," *J. Heat Transf.*, vol. 111, pp. 1045–1052, 1989.

[30] I. Mudawar and D. E. Maddox, "Critical heat flux in subcooled flow boiling of fluorocarbon liquid on a simulated electronic chip in a vertical rectangular channel," *Int. J. Heat Mass Transf.*, vol. 32, pp. 379–394, 1989.

[31] T. Y. Lee and T. W. Simon, "High-heat-flux forced convection boiling from small regions," in *Heat Transfer in Electronics*, R. K. Shah, Ed. New York: ASME, 1989, vol. 111, pp. 7–16.

[32] K. R. Samant and T. W. Simon, "Heat transfer from a small heated region to R-113 and FC-72," *ASME J. Heat Transf.*, vol. 111, pp. 1053–1059, 1989.

[33] T. C. Willingham and I. Mudawar, "Channel height effects on forced-convection boiling and critical heat flux from a linear array of discrete heat sources," *Int. J. Heat Mass Transf.*, vol. 35, pp. 1865–1880, 1992.

[34] ——, "Forced-convection boiling and critical heat flux from a linear array of discrete heat sources," *Int. J. Heat Mass Transf.*, vol. 35, pp. 2879–2890, 1992.

[35] C. O. Gersey, T. C. Willingham, and I. Mudawar, "Design parameters and practical considerations in the two-phase forced-convection cooling of multichip modules," *ASME J. Electron. Packag.*, vol. 114, pp. 280–289, 1992.

[36] W. R. McGillis, V. P. Carey, and B. D. Strom, "Geometry effects on critical heat flux for subcooled convective boiling from an array of heated elements," *ASME J. Heat Transf.*, vol. 113, pp. 463–471, 1991.

[37] C. O. Gersey and I. Mudawar, "Nucleate boiling and critical heat flux from protruded chip arrays during flow boiling," *ASME J. Electron. Packag.*, vol. 115, pp. 78–88, 1993.

[38] ——, "Effects of orientation on critical heat flux from chip arrays during flow boiling," *ASME J. Electron. Packag.*, vol. 114, pp. 290–299, 1992.

[39] ——, "Orientation effects on critical heat flux from discrete, in-line heat sources in a flow channel," *ASME J. Heat Transf.*, vol. 115, pp. 973–985, 1993.

[40] R. J. Simoneau and F. F. Simon, "A visual study of velocity and buoyancy effects on boiling nitrogen," NASA, Technical Note TN D-3354, 1966.

[41] W. R. Gambil, "Burnout in boiling heat transfer—Part II: Subcooled forced-convection systems," *Nucl. Safety*, vol. 9, pp. 467–480, 1968.

[42] K. Mishima and H. Nishihara, "The effect of flow direction and magnitude on chf for low pressure water in thin rectangular channels," *Nucl. Eng. Design*, vol. 86, pp. 165–181, 1985.

[43] T. G. Hughes and D. R. Olson, "Critical heat fluxes for curved surfaces during subcooled flow boiling," in *Proc. Nat. Heat Transf. Conf.*, vol. 3, San Francisco, CA, 1975, pp. 122–130.

[44] P. S. Wu and T. W. Simon, "Subcooled flow boiling over a thin, low-capacitance surface on a concave wall," in *Proc. Nat. Heat Transf. Conf.*, vol. 12, Portland, Oregon, 1995, pp. 177–184.

[45] J. E. Galloway and I. Mudawar, "A theoretical model for flow boiling CHF from short concave heaters," *ASME J. Heat Transf.*, vol. 117, pp. 698–707, 1995.

[46] W. R. Gambill and N. D. Green, "Boiling burnout with water in vortex flow," *Chemical Eng. Progr.*, vol. 54, pp. 68–76, 1958.

[47] C. B. Gu, L. C. Chow, and J. E. Beam, "Flow Boiling in a Curved Channel," in *Heat Transfer High Energy/High Heat Flux Applications*, R. J. Goldstein, L. C. Chow, and E. E. Anderson, Eds. New York: ASME, 1989, vol. 119, pp. 25–32.

[48] J. C. Sturgis and I. Mudawar, "Critical heat flux in a long, curved channel subjected to concave heating," *Int. J. Heat Mass Transf.*, vol. 42, pp. 3831–3848, 1999.

[49] ——, "Assessment of CHF enhancement mechanisms in a curved, rectangular channel subjected to concave heating," *ASME J. Heat Transf.*, vol. 121, pp. 394–404, 1999.

[50] D. B. Tuckerman and R. F. W. Pease, "High-performance heat sinking for VLSI," *IEEE Electron Device Lett.*, vol. 2, pp. 126–129, 1981.

[51] M. B. Bowers and I. Mudawar, "Two-phase electronic cooling using mini-channel and micro-channel heat sinks—Part I. Design criteria and heat diffusion constraints," *ASME J. Electron. Packag.*, vol. 116, pp. 290–297, 1994.

[52] ——, "Two-phase electronic cooling using minichannel and microchannel heat sinks—Part II. Flow rate and pressure drop constraints," *ASME J. Electron. Packag.*, vol. 116, pp. 298–305, 1994.

[53] ——, "High flux boiling in low flow rate, low pressure drop mini-channel and micro-channel heat sinks," *Int. J. Heat Mass Transf.*, vol. 37, pp. 321–332, 1994.

[54] P. E. Jimenez and I. Mudawar, "A multikilowatt immersion-cooled standard electronic clamshell module for future aircraft avionics," *ASME J. Electron. Packag.*, vol. 116, pp. 220–229, 1994.

[55] R. J. Phillips, "Forced-convection, liquid-cooled microchannel heat sinks," M.S. thesis, Dept. Mech. Eng., Mass. Inst. Technol., Cambridge, 1987.

[56] A. P. Ornatskii and L. S. Vinyarskii, "Heat transfer crisis in a forced flow of underheated water in small-bore tubes," *High Temp.*, vol. 3, pp. 400–406, 1965.

[57] R. D. Boyd, "Subcooled water flow boiling experiments under uniform high heat flux conditions," *Fusion Tech.*, vol. 13, pp. 131–142, 1988.

[58] ——, "Subcooled water flow boiling at 1.66 MPa under uniform high heat flux conditions," *Fusion Tech.*, vol. 16, pp. 324–330, 1989.

[59] G. P. Celata, M. Cumo, and A. Mariani, "Burnout in highly subcooled water flow boiling in small diameter tubes," *Int. J. Heat Mass Transf.*, vol. 36, pp. 1269–1285, 1993.

[60] C. L. Vandervort, A. E. Bergles, and M. K. Jensen, "An experimental study of critical heat flux in very high heat flux subcooled boiling," *Int. J. Heat Mass Transf.*, vol. 37, no. Suppl. 1, pp. 161–173, 1994.

[61] I. Mudawar and M. B. Bowers, "Ultra-high critical heat flux (CHF) for subcooled water flow boiling -I. CHF data and parametric effects for small diameter tubes," *Int. J. Heat Mass Transf.*, vol. 42, pp. 1405–1428, 1999.
[62] D. D. Hall and I. Mudawar, "Ultra-high critical heat flux (CHF) for subcooled water flow boiling—II. High-CHF database and design parameters," *Int. J. Heat Mass Transf.*, vol. 42, pp. 1429–145, 1999.
[63] Y. Katto and M. Kunihiro, "Study of the mechanism of burnout in boiling system of high burnout heat flux," *Bull. JSME*, vol. 16, pp. 1357–1366, 1973.
[64] M. Katsuta, "Boiling heat transfer of thin liquid with an impinging jet," in *Proc. 14th Nat. Heat Transf. Symp. Jpn.*, 1977, pp. 154–156.
[65] M. Monde and Y. Katto, "Burnout in a high heat-flux boiling system with an impinging jet," *Int. J. Heat Mass Transf.*, vol. 21, pp. 295–305, 1978.
[66] M. Monde, "Critical heat flux in saturated forced convection boiling on a heated disk with an impinging jet," *ASME J. Heat Transf.*, vol. 109, pp. 991–996, 1987.
[67] K. A. Estes and I. Mudawar, "Comparison of Two-Phase Electronic Cooling using Free Jets and Sprays," *ASME J. Electron. Packag.*, vol. 117, pp. 323–332, 1995.
[68] I. Mudawar and D. C. Wadsworth, "Critical heat flux from a simulated electronic chip to a confined rectangular impinging jet of dielectric liquid," *Int. J. Heat Mass Transf.*, vol. 34, pp. 1465–1480, 1991.
[69] L. H. J. Watchers, L. Smulders, J. R. Vermeulen, and H. C. Kleiweg, "The heat transfer from a hot wall to impinging mist droplets in the spheroidal state," *Chem. Eng. Sci.*, vol. 21, pp. 1231–1238, 1966.
[70] L. Bolle and J. C. Moureau, "Spray cooling of hot surfaces: A description of the dispersed phase and a parametric study of heat transfer results," in *Proc. Two Phase Flow Heat Transf., Adv. Study Inst.*, vol. 3, Washington, D.C, 1976, pp. 1327–1346.
[71] A. Moriyama, K. Araki, M. Yamagami, and K. Mase, "Local heat transfer coefficient in spray cooling a hot surface," in *Proc. 15th Jpn. Conf. Liquid Atomization Spray Syst.*, vol. 28, Tokyo, Japan, 1987, pp. 104–109.
[72] S. Toda, "A Study in mist cooling," *Trans. JSME*, vol. 38, pp. 581–588, 1972.
[73] I. Mudawar and W. S. Valentine, "Determination of the local quench curve for spray-cooled metallic surfaces," *ASM J. Heat Treating*, vol. 7, pp. 107–121, 1989.
[74] I. Mudawar and T. A. Deiters, "A universal approach to predicting temperature response of metallic parts to spray quenching," *Int. J. Heat Mass Transf.*, vol. 37, pp. 347–362, 1994.
[75] K. A. Estes and I. Mudawar, "Correlation of sauter mean diameter and chf for spray cooling of small surfaces," *Int. J. Heat Mass Transf.*, vol. 38, pp. 2985–2996, 1995.
[76] I. Mudawar and K. A. Estes, "Optimizing and predicting CHF in spray cooling of a square surface," *ASME J. Heat Transf.*, vol. 118, pp. 672–679, 1996.
[77] D. E. Tilton and C. L. Tilton, "High heat flux spray cooling," U.S. Patent 5 220 804, 1993.
[78] D. D. Hall and I. Mudawar, "Experimental and numerical study of quenching complex-shaped metallic alloys with multiple, overlapping sprays," *Int. J. Heat Mass Transf.*, vol. 38, pp. 1201–1216, 1995.
[79] M. Mackowski, "Requirements for high flux cooling of future avionics systems," in *Proc. SAE Conf.*, 1991.
[80] M. Barwick, M. Midkoff, and D. Seals, "Liquid flow-through cooling for avionics applications," in *Proc. IEEE 1991 Nat. Aerosp. Electron. Conf. (NAECON)*, vol. 1, Dayton, OH, 1991, pp. 227–230.
[81] I. Mudawar, P. E. Jimenez, and R. E. Morgan, "Immersion-cooled standard electronic clamshell module: A building block for future high-flux avionic systems," *ASME J. Electron. Packag.*, vol. 116, pp. 116–125, 1994.
[82] M. E. Johns and I. Mudawar, "An ultra-high power two-phase jet-impingement avionic clamshell module," *ASME J. Electron. Packag.*, vol. 118, pp. 264–270, 1996.

Issam Mudawar received the M.S. and Ph.D. degrees from the Massachusetts Institute of Technology, Cambridge, in 1980 and 1984, respectively.

His graduate work involved magnetohydrodynamic (MHD) energy conversion and phase-change water cooling of turbine blades. He joined the School of Mechanical Engineering, Purdue University, West Lafayette, IN, in 1984, where he established and became Director of the Boiling and Two-Phase Flow Laboratory (BTPFL) and Electronic Cooling Research Center (ECRC). His work has been focused on phase change processes, thermal management of electronic and aerospace devices, intelligent materials processing, and nuclear reactor safety. His theoretical and experimental research encompasses sensible and evaporative heating of thin films, pool boiling, flow boiling, jet-impingement cooling, spray cooling, micro-channel heat sinks, heat transfer enhancement, heat transfer in rotating systems, critical heat flux, capillary pumped flows, and surface rewetting. His Electronic Cooling Research Center was renamed in 1998 as the Purdue University International Electronic Cooling Alliance (PUIECA), where efforts are presently focussed entirely on high-heat-flux cooling schemes. He presently serves as Chairman of the Heat Transfer Area at Purdue University. He is also President of Mudawar Thermal Systems, Inc., a firm that is dedicated to the development of thermal solutions to computer and aerospace problems.

Dr. Mudawar received the Best Paper Award in Electronic Cooling at the 1988 National Heat Transfer Conference, the Best Paper Award in Thermal Management at the 1992 ASME/JSME Joint Conference on Electronic Packaging, the *Journal of Electronic Packaging* Outstanding Paper of the Year Award for 1995, the Solberg Award for Best Teacher in School of Mechanical Engineering (1987, 1992, and 1996), Charles Murphy Award for Best Teacher at Purdue University (1997), and the National Society of Black Engineers Professor of the Year Award (1985, 1987). He is a Fellow of the American Society of Mechanical Engineers.